isvr Institute of Sound and Vibration Research

Velocity Feedback Control of Vibration Isolation Systems

B. Yan, M.J. Brennan, S.J. Elliott and N.S. Ferguson

ISVR Technical Memorandum No 962

March 2006

University of Southampton

SCIENTIFIC PUBLICATIONS BY THE ISVR

Technical Reports are published to promote timely dissemination of research results by ISVR personnel. This medium permits more detailed presentation than is usually acceptable for scientific journals. Responsibility for both the content and any opinions expressed rests entirely with the author(s).

Technical Memoranda are produced to enable the early or preliminary release of information by ISVR personnel where such release is deemed to the appropriate. Information contained in these memoranda may be incomplete, or form part of a continuing programme; this should be borne in mind when using or quoting from these documents.

Contract Reports are produced to record the results of scientific work carried out for sponsors, under contract. The ISVR treats these reports as confidential to sponsors and does not make them available for general circulation. Individual sponsors may, however, authorize subsequent release of the material.

UNIVERSITY OF SOUTHAMPTON

INSTITUTE OF SOUND AND VIBRATION RESEARCH

DYNAMICS GROUP

Velocity Feedback Control of Vibration Isolation Systems

by

B. Yan, M.J. Brennan, S.J. Elliott and N.S. Ferguson

ISVR Technical Memorandum No: 962

March 2006

Authorised for issue by
Professor M.J. Brennan
Group Chairman

Abstract

The isolation of sensitive equipment from the vibration of a base structure to which it is attached, is required in many application areas. Such isolation is usually achieved using resilient mount. A conventional passive isolation system consists of a compliant mount positioned between the base structure and the equipment to be isolated. However, such passive systems suffer from a trade-off between low- and high-frequency isolation performances, depending on the damping of the mount. This compromise can be avoided using active isolation solutions.

In this report, vibration isolation systems with a lumped parameter isolator and the use of velocity feedback control on such systems have been summarized and presented based on previous work. Two different velocity feedback control methods have been applied and compared. The control performance and stability have been investigated.

In practice, it would be more accurate to treat the isolator as a continuous system, especially at relatively high frequencies, when the resonances due to the isolator might affect the isolation performance, or even destabilize the control system. Therefore, vibration isolation systems containing a distributed parameter mount have been analyzed under two different control methods. In this report, the distributed parameter isolator represented by an elastic rod, which itself has distributed mass and stiffness. The control performances of such systems have been investigated and compared. The stability has also been discussed.

List of contents

List of figures

Section 2

Section 3

Appendix

List of symbols

c_m	Viscous damping constant of the lumped parameter isolator
E	Young's modulus of elasticity of the rod
E^*	Complex Young's modulus of elasticity of the rod
f	Primary excitation force applied on the base
f_a	Control force generated by the actuator
f_b	External force applied on the base structure
f_e	External force applied on the equipment
$f_m\, f_{m1}\, f_{m2}$	Reactive force generated by the isolator
f_s	Force applied at the excitation point s for a multi-degree-of freedom system
$f_1\, f_2$	Force applied on the isolator
G	Plant frequency response function
G^{-1}	Reciprocal of plant frequency response function
h	Feedback gain
$h_{\max}$	Maximum feedback gain
k_a	Stiffness of the additional system
k_b	Stiffness of the base structure
k_b^*	Complex stiffness of the base structure
k_e	Stiffness of the equipment
K_j	Modal stiffness of the j^{th} mode of a multi-degree-of freedom system
k_l	Longitudinal wave number of the rod
k_l^*	Complex longitudinal wave number of the rod
k_m	Stiffness of isolator
k_s	Static stiffness of the finite free-free rod
k_t	Total stiffness of the mount and equipment

L	Length of the finite free-free rod
m_a	Mass of the additional system
m_b	Mass of base structure
m_e	Mass of equipment
M_j	Modal mass of the j^{th} mode of a multi-degree-of freedom system
P_{f_a}	Time averaged power generated by the control force
S	Cross-sectional area of the finite free-free rod
S_b	Power spectral densities of the base disturbance
S_e	Power spectral densities of the equipment response
T	Transmissibility function
$\|T\|_{\max}$	Maximum of the transmissibility function
$\|T\|_{\min}$	Minimum of the transmissibility function
$\|T\|_{lightrod}$	Transmissibility of the system with a massless rod as the isolator
v_b	Velocity of the base structure at the mount junction
v_b^*	Conjugate of the base velocity at the mount junction
v_e	Velocity of the equipment at mount junction
v_e^*	Conjugate of the equipment velocity at mount junction
$\overline{v_e^2}$	Mean square response of the equipment
v_r	Velocity at the response point *r* for a multi-degree-of freedom system
x	Displacement of the equipment at mount junction
Y	Mobility
Y_b	Input mobility of the unconnected base structure
Y_e	Input mobility of the unconnected equipment
Y_{bb}	Input mobility of the base when coupled to the rest of the system

Y_{eb}	Transfer mobility from the force excitation on the base structure to the equipment velocity when the system is coupled
Y_{ee}	Input mobility of the equipment when coupled to the rest of the system
Z_m	Impedance of the isolator
$\mathbf{Z}_r$	Impedance matrix of the finite free-free rod
Z_{11} Z_{22}	Point impedance of the finite free-free rod
Z_{12} Z_{21}	Transfer impedance of the finite free-free rod
δ_{st}	Static deflection of the base structure
$\phi_b^{(j)}$	The j^{th} mode shape evaluated at the base structure
$\phi_e^{(j)}$	The j^{th} mode shape evaluated at the equipment
$\phi_r^{(j)}$	The j^{th} mode shape evaluated at the response point r of a multi-degree-of freedom system
$\phi_s^{(j)}$	The j^{th} mode shape evaluated at the excitation point s of a multi-degree-of freedom system
Γ_b	Natural frequency ratio of the base structure to the equipment
ω	Frequency in radius per second
ω_b	Natural frequency of the base structure in radius per second
ω_e	Natural frequency of the mounted equipment in radius per second
ω_j	The j^{th} natural frequency of a multi-degree-of freedom system in radius per second
Ω_e	Non-dimensional frequency
Ω_j	Non-dimensional frequency of the j^{th} mode of a multi-degree-of freedom system
η_b	Loss factor in the base structure
η_m	Loss factor in the rod
μ_b	Mass ratio of base to the equipment
μ_m	Mass ratio of isolator to the equipment

μ_k	Stiffness ratio of isolator to the base structure
ρ	Density of the rod
ζ_a	Active damping ratio due to the control
ζ_j	Modal damping ratio of the j^{th} mode of a multi-degree-of freedom system
ζ_m	Passive damping ratio in the isolator

List of Abbreviations

AVF	Absolute velocity feedback
RVF	Relative velocity feedback

1. Introduction

For delicate equipment attached to a vibrating host base structure, there is a need for vibration isolation. This is often achieved using passive isolators such as rubber mountings. A conventional passive isolation system consists of a compliant mount positioned between the base structure and the equipment to be isolated, and this can provide good isolation at high frequencies well above the resonance caused by the mass of the equipment and the stiffness of the mount [1]. However, conventional passive isolation systems suffer from a trade-off in the choice of their damping [2-4]. If the passive isolator damping is too small, the equipment vibration is amplified compared with the base vibration close to the mounted natural frequency. If the passive isolator damping is too large, the vibration transmissibility is increased at frequencies well above the mounted natural frequency compared to the case of low damping and also the rate of reduction with frequency is less. This trade-off is illustrated and introduced in section 2.2.1. Also, in space, rubber mounts have limited application because of their temperature dependence [5]. Consequently passive metallic vibration isolators have to be used, but these have inherently light damping that causes vibration amplification at some frequencies. The compromises inherent in using a passive system can be avoided using active vibration isolation system with feedback control [6]. This active method of controlling the response at the resonance frequency is to use a feedback controller to generate a secondary force which is proportional to the absolute velocity of the equipment. It is sometimes referred to as skyhook damping if it reacts off the base structure [7].

In the conventional analysis of the dynamics of vibration isolation, the passive compliant mount, which is usually modelled as the combination of an elastic spring and a viscous damper, is assumed to behave as a lumped parameter system. Much previous research work has been done in reducing vibration transmission from a vibrating base to a mounted equipment structure with a lumped parameter isolator, under feedback control, in which cases, the active mount is modelled as a single-axis force actuator in parallel with the passive isolator [7, 8]. The feedback sensor measures either the absolute velocity of the equipment to be isolated at one end of the mount, or the integral of the transmitted force through the mount. The plant response,

from force actuator input to sensor output, is derived in terms of the mechanical mobilities of the two structures connected by the active mount. The stability and performance of the analytic models with the lumped parameter isolator has been analyzed and the experiment of multi-channel direct velocity feedback control has been performed with both reactive and inertial actuators. The effect of equipment and base flexibility on these systems and the global effect of local controllers in such systems have also been analyzed. In the absence of actuator and sensor dynamics, the integrated force feedback system is unconditionally stable. The stability of the absolute velocity feedback system is, however, threatened if the vibrating base structure becomes very mobile, with a small effective mass, at the same frequency where the equipment structure becomes dynamically very stiff [8, 9]. However, it would be more accurate to treat the mount as a continuous system, especially at relatively high frequencies, when the resonances due to the mount might affect the stability of the control system.

This report describes analytical and numerical modelling of active isolation systems containing either a lumped parameter isolator or a distributed parameter mount together with controller design and stability analysis.

In section 2, the review work on vibration isolation systems with a lumped parameter isolator reducing vibration transmission from a vibrating base to a mounted equipment structure are presented and summarized. Control performance and the stability of these systems under absolute velocity feedback control and relatively velocity feedback control are investigated and compared.

.

In section 3, the analytical models with a distributed parameter isolator are then introduced and analyzed. Also, control performance and the stability of the systems under absolute velocity feedback control and relatively velocity feedback control are investigated and compared.

Overall conclusions are presented in section 4.

2. Vibration isolation systems with a lumped parameter isolator

2.1 Introduction

Vibration isolation systems with a lumped parameter isolator have been investigated by many researchers. Serrand [8] and Elliott et al [9] have analyzed such dynamic systems using mobility approach. The stability for such systems under absolute velocity feedback control has also been discussed by looking at their plant responses [7, 9]. In this section, previous work on vibration isolation systems with a lumped parameter isolator has been summarized and presented. Furthermore, relative velocity feedback control is applied to such systems. The stability is investigated and control performance is analyzed and compared with absolute velocity feedback control.

2.2 A vibration isolation system with a lumped parameter isolator undergoing harmonic base motion

Vibrating systems with a lumped parameter isolator undergoing harmonic base motion are analyzed in this section. The frequency response of the passive system is investigated and two different control strategies are applied.

2.2.1 Passive system

A vibrating system with a lumped parameter isolator, which is modelled as an elastic spring and a viscous damper in parallel, undergoing harmonic base motion is modelled as in Figure 2.1. The equations of motion in terms of mobility/impedance are given by

$$\begin{aligned} v_e &= Y_e\left(f_e + f_m\right) \\ f_m &= -f_2 \\ \begin{bmatrix} f_1 \\ f_2 \end{bmatrix} &= \begin{bmatrix} Z_m & -Z_m \\ -Z_m & Z_m \end{bmatrix} \begin{bmatrix} v_b \\ v_e \end{bmatrix} \end{aligned} \qquad (2.1\text{a,b,c})$$

where Y_e is the input mobility of the unconnected equipment at the location of the mount connection, Z_m is the impedance of the mount which characterises the mount properties and $Z_m = k_m / j\omega + c_m$.

The velocity of the equipment is given by

$$v_e = \frac{Y_e}{1+Y_e Z_m} f_e + \frac{Y_e Z_m}{1+Y_e Z_m} v_b \tag{2.2}$$

Without the external force f_e exciting on the equipment, the transmissibility can be written as

$$T = \frac{v_e}{v_b} = \frac{Y_e Z_m}{1+Y_e Z_m} \tag{2.3}$$

In Figure 2.1, if the equipment is modelled as a mass, so that $Y_e = 1/j\omega m_e$, the transmissibility can be written in terms of non-dimensional parameters as

$$T = \frac{k_m + j\omega c_m}{k_m - \omega^2 m_e + j\omega c_m} = \frac{1+j2\zeta_m \Omega_e}{1-\Omega_e^2 + j2\zeta_m \Omega_e} \tag{2.4}$$

where $\Omega_e = \omega / \omega_e$ and $\omega_e = \sqrt{k_m / m_e}$ is the natural frequency of the equipment mass on the stiffness. $\zeta_m = c_m / 2\sqrt{k_m m_e}$ is the viscous damping ratio.

Figure 2.2 shows the transmissibility with different values of damping ratio ζ_m. If the damping ratio is very small ($\zeta_m << 1$), at relatively high frequency well above the mounted natural frequency, the transmissibility reduces at 40 dB/decade before it eventually rolls off at 20 dB/decade. Otherwise, if the damping ratio is relatively large, at high frequency the transmissibility reduces at 20 dB/decade, although the isolation performance is much better around the resonance frequency than when the damping ratio is small.

This reveals an important issue in vibration isolation. Conventional passive systems for the isolation of equipment from base vibration involve an inherent compromise between good high frequency isolation, which requires small values of isolator damping, and low vibration amplitudes at frequencies close to the mounted natural frequency, which requires large values of isolator damping [2-4].

2.2.2 The system under Absolute Velocity Feedback control

Figure 2.3 shows the system under absolute velocity feedback (AVF) control. A control actuator, which is in parallel with the passive isolator, reacts between the equipment and the base.

- **Control performance**

Substituting the control force, f_a for the external force, f_e, equation (2.2) can be rewritten as

$$v_e = \frac{Y_e}{1+Y_eZ_m} f_a + \frac{Y_eZ_m}{1+Y_eZ_m} v_b \tag{2.5}$$

The control force f_a which is proportional to the velocity of the suspended mass is fed back to the system with a gain -*h*, which is a constant, so that

$$f_a = -hv_e \tag{2.6}$$

Substituting equation (2.6) into (2.5), the transmissibility under AVF control is given by

$$T = \frac{Y_eZ_m}{1+Y_eZ_m+hY_e} \tag{2.7}$$

If the equipment is modelled as a mass, the equation (2.7) can be written in terms of non-dimensional parameters as

$$T = \frac{k_m + j\omega c_m}{k_m - \omega^2 m_e + j\omega(c_m+h)} = \frac{1+j2\zeta_m\Omega_e}{1-\Omega_e^2 + j2\Omega_e(\zeta_m+\zeta_a)} \tag{2.8}$$

where $\zeta_a = h/2\sqrt{k_m m_e}$ is the damping ratio due to the feedback control.

The feedback adds a damping term to the denominator and leaves the numerator unchanged. The action of absolute velocity feedback is the same as a passive viscous damper acting between the payload and a fixed motionless base as illustrated by Figure 2.4, which is known as 'skyhook damping' [7].

Figure 2.5 shows the transmissibility for the system with a fixed passive damping ratio ζ_m and different values of active damping ratio ζ_a. It can be noted that the resonance peak is significantly suppressed with an increase in the active damping ratio while the performances at relatively high frequencies above the natural frequency of the mounted equipment is not affected. Hence, active vibration isolation

with an active controller using the absolute velocity response of the mounted equipment offers a way of overcoming the inherent compromise in the choice of damping in the conventional passive systems.

- **Stability analysis**

The Nyquist criterion states that for a stable open-loop system the closed-loop system is also stable provided the Nyquist contour does not enclose the unstable point (-1, j0) [10-12]. In this study, the controller is a simple constant gain h so that the Nyquist analysis of the open-loop frequency response can be reduced to the consideration of the plant response considering a unitary control gain (h=1).

For the vibrating system with a lumped parameter isolator under AVF control shown in Figure 2.3, the plant response from actuator force to absolute equipment velocity is given by

$$G = \frac{Y_e}{1 + Y_e Z_m} = \frac{1}{Z_e + Z_m} \tag{2.9}$$

where Z_e is the input impedance of the unconnected equipment at the location of the mount connection.

The stability can be analyzed by examining the reciprocal of the plant response, which is

$$G^{-1} = Z_e + Z_m \tag{2.10}$$

Z_e is an input impedance, so that its phase is between -90° and 90°. The phase of Z_m will be -90° if the mount is dominated by its stiffness, reducing to 0° if it is dominated by its damping. Therefore the overall phase of G^{-1} could range between -90° and 90°. The phase limitations on the plant response G from actuator force to absolute equipment velocity are thus given by

$$-90^0 < \angle G < 90^0 \tag{2.11}$$

The absolute value of the phase of the plant response is never greater than π so that the Nyquist plot of the plant response never crosses the negative real axis. Therefore, based on the Nyquist criterion, the system is unconditionally stable.

2.2.3 The system under Relatively Velocity Feedback control

Figure 2.6 shows the system under relative velocity feedback (RVF) control. A control actuator, which is in parallel with the passive isolator, reacts between the equipment and the base.

- **Control performance**

The control force f_a which is proportional to the difference between absolute equipment velocity and absolute base velocity is fed back to the system with a gain *-h*, so that

$$f_a = -h\left(v_e - v_b\right) \tag{2.12}$$

Substituting the equation (2.12) into (2.5), the transmissibility under RVF control is given by

$$T = \frac{Y_e Z_m + hY_e}{1 + Y_e Z_m + hY_e} \tag{2.13}$$

If the equipment has a mass-like mobility, equation (2.13) can be written as

$$T = \frac{k_m + j\omega\left(c_m + h\right)}{k_m - \omega^2 m_e + j\omega\left(c_m + h\right)} = \frac{1 + j2\Omega_e\left(\zeta_m + \zeta_a\right)}{1 - \Omega_e^2 + j2\Omega_e\left(\zeta_m + \zeta_a\right)} \tag{2.14}$$

The feedback adds a damping term both to the denominator and the numerator. The action of relative velocity feedback is equivalent to a passive viscous damper acting between the equipment and the base as illustrated by Figure 2.7. Therefore, the system under RVF control still involves an inherent compromise between good high frequency isolation and low resonance peak at the mounted natural frequency, as shown in Figure 2.8.

The comparison of the control performance between the system under RVF and AVF control can be realized by looking at their change in mean square response compared to the original passive system. The relationship between the power spectral densities of the base disturbance and equipment response can be written as

$$S_e = |T|^2 S_b \tag{2.15}$$

where S_e and S_b are the power spectral densities of the base disturbance and equipment response, respectively. T is the transmissibility discussed in former sections.

The mean square response of the equipment is thus given by

$$\overline{v_e^2} = \int_{-\infty}^{+\infty} S_e d\Omega_e = \int_{-\infty}^{+\infty} |T|^2 S_b d\Omega_e \tag{2.16}$$

For the systems without and with AVF and RVF control, substituting the corresponding transmissibility, the change in the mean square response for the system under AVF and RVF control compared to the original passive system can be calculated.

Figure 2.9 depicts the change in mean square velocity compared to the original passive system. At high active damping ratios, the AVF control provides increasing reduction in the mean square response. The performance of the RVF control system is always worse than the performance of the AVF control system and does not produce monotonically reducing mean square response for an increase in active damping ratio.

- **Stability analysis**

For the vibrating system with a lumped parameter isolator under RVF control shown in Figure 2.6, the plant response from actuator force to the difference between absolute equipment velocity and absolute base velocity is given by

$$G = \frac{Y_e}{1 + Y_e Z_m} = \frac{1}{Z_e + Z_m} \tag{2.17}$$

It is the same as the plant response for such a system under AVF control. Therefore, its phase ranges between -90° and 90° so that the system is unconditionally stable.

2.2.4 Conclusions

The action of absolute velocity feedback on a system with a lumped parameter isolator undergoing harmonic base motion is the same as a skyhook damper, which offers a way of overcoming the inherent compromise in the choice of damping in the conventional passive systems. Moreover, the system is unconditionally stable.

The action of relative velocity feedback on such a system is the same as a passive viscous damper acting between the equipment and the base, which is also unconditionally stable. However, its control performance is worse than that of the system under AVF control, especially at high damping ratios due to the control.

2.3 A vibration isolation system with a lumped parameter isolator on a flexible base

A vibrating system with a lumped parameter isolator on a flexible base is analyzed in this section. The frequency response of the system is studied and two different control strategies are applied and compared.

2.3.1 Passive system

A vibrating system with a lumped parameter isolator on a flexible base is modelled as in Figure 2.10. The equations of motion are given by

$$\begin{aligned} v_e &= Y_e\left(f_e + f_{m2}\right) \\ v_b &= Y_b\left(f_b + f_{m1}\right) \\ \begin{bmatrix} f_{m1} \\ f_{m2} \end{bmatrix} &= -\begin{bmatrix} f_1 \\ f_2 \end{bmatrix} = -\begin{bmatrix} Z_m & -Z_m \\ -Z_m & Z_m \end{bmatrix}\begin{bmatrix} v_b \\ v_e \end{bmatrix} \end{aligned} \qquad (2.18a,b,c)$$

where Y_b is the input mobility of the unconnected base at the location of the mount connection.

The velocity of the equipment can be written as

$$v_e = Y_{ee} f_e + Y_{eb} f_b \qquad (2.19)$$

and

$$Y_{ee} = \frac{Y_e\left(1 + Y_b Z_m\right)}{1 + Z_m\left(Y_e + Y_b\right)} \qquad (2.20)$$

$$Y_{eb} = \frac{Y_e Y_b Z_m}{1 + Z_m\left(Y_e + Y_b\right)} \qquad (2.21)$$

where Y_{ee} is the input mobility of the equipment when coupled to the rest of the system and Y_{eb} is the transfer mobility from the force on the base, f_b to the equipment velocity, v_e when the system is coupled [7, 8].

If the system is only excited by the external force on the base, $f_b = f$, i.e. external force $f_e = 0$, the velocity of the equipment can be written as

$$\frac{v_e}{f} = Y_{eb} = \frac{Y_e Y_b Z_m}{1 + Z_m (Y_e + Y_b)} \tag{2.22}$$

If the equipment has a mass-like mobility and the base structure is modelled as a mass m_b on a complex spring, i.e. $k_b^* = k_b(1 + j\eta_b)$, where η_b is the loss factor, the non-dimensional amplitude ratio can be written as

$$\frac{x}{\delta_{st}} = \frac{1 + j2\zeta_m \Omega_e}{1 + \Omega_e^2 \left[\frac{\Omega_e^2}{\Gamma_b^2} - 1 - \left(1 + \frac{1}{\mu_b}\right)\frac{1}{\Gamma_b^2} \right] - 2\zeta_m \eta_b \Omega_e + j\left\{ \eta_b \left(1 - \Omega_e^2\right) + 2\zeta_m \Omega_e \left[1 - \left(1 + \frac{1}{\mu_b}\right)\right]\frac{\Omega_e^2}{\Gamma_b^2} \right\}} \tag{2.23}$$

where x is the displacement of the equipment, $\delta_{st} = f / k_b$ is the static deflection of the base, $\omega_b = \sqrt{k_b / m_b}$ is the natural frequency of the base, $\Gamma_b = \omega_b / \omega_e = 1/\sqrt{\mu_k \mu_b}$ is the natural frequency ratio, $\mu_k = k_m / k_b$ is the stiffness ratio, $\mu_b = m_b / m_e$ is the mass ratio of the supporting base structure to the mounted equipment.

Figure 2.11 shows the amplitude ratio of the system with different values of the passive damping ratio ζ_m and loss factor η_b. It can be seen that the damping in the base structure is only beneficial to the reduction of the peak broadly due to the base dynamics, which is the second peak in Figure 2.11. The damping in the lumped parameter isolator is effective in reducing both resonance peaks; however, the amplitude ratio is amplified at high frequencies above the base dominated resonance.

2.3.2 The system under Absolute Velocity Feedback control

Figure 2.12 shows the system configuration under absolute velocity feedback control.

- **Control performance**

Referring to the description in section 2.2.1, the external force and control forces acting on the base and equipment respectively are given by

$$f_e = f_a \tag{2.24}$$

$$f_b = f - f_a \tag{2.25}$$

Substituting them into Equation (2.19), the equipment velocity can be written as

$$v_e = \left(Y_{ee} - Y_{eb}\right) f_a + Y_{eb} f \tag{2.26}$$

Substituting equation (2.6) into (2.26), the equipment velocity under AVF control is given by

$$\frac{v_e}{f} = \frac{Y_{eb}}{1+h\left(Y_{ee}-Y_{eb}\right)} = \frac{Y_e Y_b Z_m}{1+Z_m\left(Y_e+Y_b\right)+hY_e} \tag{2.27}$$

If the equipment has a mass-like mobility and the base structure is modelled as a mass on a complex spring, the amplitude ratio of the system under AVF control can be written as

$$\frac{x}{\delta_{st}} = \frac{1+j2\zeta_m\Omega_e}{1+\Omega_e^2\left[\frac{\Omega_e^2}{\Gamma_b^2}-1-\left(1+\frac{1}{\mu_b}\right)\frac{1}{\Gamma_b^2}\right]-2\left(\zeta_m+\zeta_a\right)\eta_b\Omega_e} \cdots$$

$$\cdots \frac{}{+j\left\{\eta_b\left(1-\Omega_e^2\right)+2\zeta_m\Omega_e\left[1-\left(1+\frac{1}{\mu_b}\right)\right]\frac{\Omega_e^2}{\Gamma_b^2}+2\zeta_a\Omega_e\left(1-\frac{\Omega_e^2}{\Gamma_b^2}\right)\right\}} \tag{2.28}$$

The feedback adds a damping term to the denominator and leaves the numerator unchanged. Figure 2.13 shows the amplitude ratio for the system with different values of damping ratio ζ_a due to feedback control. The equipment and base resonance peaks are both attenuated with an increase in the active damping ratio, while the performance at high frequencies well above the natural frequencies is unaltered.

- **Stability analysis**

For the vibrating system on a flexible base under AVF control shown in Figure 2.12 the plant response from actuator force to absolute equipment velocity can be written as [9]

$$G = Y_{ee} - Y_{eb} = \frac{Y_e}{1+Z_m\left(Y_e+Y_b\right)} \tag{2.29}$$

The phase limits of the plant response are thus given by

$$-180^0 < \angle G < 270^0 \tag{2.30}$$

Therefore, the system with a constant gain feedback loop is only conditionally stable. The stability conditions for such a system have previously been discussed by Elliott et al [9]. A feedback system from absolute equipment velocity to actuator force will be unconditionally stable unless every one of the following conditions is simultaneously satisfied at some frequency:

(1) The equipment dynamics are stiffness-dominated, so that $Y_e(j\omega) = j\omega/k_e$ and $k_e > 0$,

(2) The base dynamics are mass-dominated, so that $Y_b(j\omega) = 1/j\omega m_b$ and $m_b > 0$,

(3) The stability parameter is greater than unity; $k_t / \omega^2 m_b > 1$, where $k_t = k_m k_e /(k_m + k_e)$.

Figure 2.14 shows a system with a lumped parameter isolator on a flexible base which can be unstable at some frequencies. If appropriate parameters for the addition mass, m_a, and stiffness, k_a, attached to the equipment are chosen so that these three conditions are satisfied, then the system becomes unstable [9]. Figures 2.15 and 2.16 show the frequency response and Nyquist plot of the plant response G of an unstable case for the system shown in Figure 2.14. The parameters chosen are $m_a = 3.5$ kg, $m_e = 1.7$ kg, $m_b = 1.1$ kg, $k_a = k_m = 12{,}000$ N/m and $c_m = 33$ Ns/m. In the complex plane there is a loop on the left half of the complex plane. With an increase in the control gain, this will eventually enclose the point (-1, j0) and this corresponds to the system becoming unstable. Figure 2.17 shows the open and closed-loop response from a force on the base structure to the equipment velocity for the system. It can be observed that some attenuation at the mount resonance is achieved, but this is accompanied by enhancement of the velocity at the equipment resonance.

2.3.3 The system under Relative Velocity Feedback control

Figure 2.18 shows the system with a lumped parameter isolator on a flexible base under relative velocity feedback control.

- **Control performance**

Substituting equation (2.12) into (2.26), and because

$$v_b = (Y_{eb} - Y_{bb}) f_a + Y_{bb} f \tag{2.31}$$

The equipment velocity under RVF control is given by

$$\frac{v_e}{f} = \frac{Y_{eb} + h(Y_{ee}Y_{bb} - Y_{eb}^2)}{1 + h(Y_{ee} + Y_{bb} - 2 \cdot Y_{eb})} \tag{2.32}$$

where Y_{bb}, which is the input mobility of the base when coupled to the rest of the system, is given as

$$Y_{bb} = \frac{Y_b(1 + Y_e Z_m)}{1 + Z_m(Y_b + Y_b)} \tag{2.33}$$

Therefore, equation (2.32) can be rewritten as

$$\frac{v_e}{f} = \frac{Y_e Y_b Z_m + h Y_e Y_b}{1 + Z_m (Y_e + Y_b) + h(Y_e + Y_b)} \tag{2.34}$$

If the equipment has a mass-like mobility and the base structure is modelled as a mass on a complex spring, the amplitude ratio of the system under RVF control can be written as

$$\frac{x}{\delta_{st}} = \frac{1 + j2(\zeta_m + \zeta_a)\Omega_e}{1 + \Omega_e^2 \left[\frac{\Omega_e^2}{\Gamma_b^2} - 1 - \left(1 + \frac{1}{\mu_b}\right)\frac{1}{\Gamma_b^2} \right] - 2(\zeta_m + \zeta_a)\eta_b \Omega_e} \cdots$$

$$\cdots \frac{}{+ j\left\{ \eta_b \left(1 - \Omega_e^2\right) + 2(\zeta_m + \zeta_a)\Omega_e \left[1 - \left(1 + \frac{1}{\mu_b}\right) \right] \frac{\Omega_e^2}{\Gamma_b^2} \right\}} \tag{2.35}$$

The feedback adds a damping term both to the denominator and the numerator. Figure 2.19 shows the amplitude ratio for the system with different values of damping ratio due to feedback control. The resonance peaks are attenuated at high active damping ratios while the amplitude ratio is amplified between two resonance peaks and at high frequencies well above the mounted natural frequencies. Therefore its control performance is worse than that of the system under AVF control, especially at high active damping ratios.

Similar to the description in section 2.2.3, the relationship between the power spectral densities of the base disturbance and equipment response can be written as

$$S_e = \left| \frac{x}{\delta_{st}} \right|^2 S_b \tag{2.36}$$

where x/δ_{st} is the amplitude ratio discussed in former sections.

The mean square response of the equipment is thus given by

$$\overline{x^2} = \int_{-\infty}^{+\infty} S_e d\Omega_e = \int_{-\infty}^{+\infty} \left| \frac{x}{\delta_{st}} \right|^2 S_b d\Omega_e \tag{2.37}$$

Figure 2.20 depicts the change in mean square displacement compared to the original passive system. Although the behaviour is very similar to the case when the base is

rigid, the additional mode due the dynamics of the base has a negative contribution to the reduction of the mean square responses.

- **Stability analysis**

For the system under RVF control, the plant response is given by

$$G = Y_{ee} + Y_{bb} - 2Y_{eb} = \frac{Y_e + Y_b}{1 + Z_m(Y_e + Y_b)} \tag{2.38}$$

The reciprocal of the plant response is thus

$$G^{-1} = Z_m + (Y_e + Y_b)^{-1} \tag{2.39}$$

Y_e and Y_b are both input mobilities, thus have phase between -90° and 90°, so that the phase of $(Y_e + Y_b)^{-1}$ is also between -90° and 90° . The phase shift of Z_m will be -90° if the mount is dominated by its stiffness, reducing to 0° if it is dominated by its damping. Therefore the overall phase of G^{-1} could range between -90° and 90°. The phase limitations on the plant response G are thus given by

$$-90^0 < \angle G < 90^0 \tag{2.40}$$

Therefore, based on the Nyquist criterion, the system is unconditionally stable.

2.3.4 Conclusions

The action of absolute velocity feedback on a system with a lumped parameter isolator on a flexible base is similar to a skyhook damper. The resonance peaks are attenuated with an increase of the active damping ratio while the performances at relatively high frequencies above the natural frequencies are unchanged. However, such a control system is only conditionally stable.

The action of relative velocity feedback on such a system is the same as a passive viscous damper, which is unconditionally stable. The resonance peaks are attenuated at high active damping ratios while the amplitude ratio is amplified at high frequencies. Therefore, although such a system is unconditionally stable, the penalty is that its control performance is worse than that of the system under AVF control, especially at high active damping ratios.

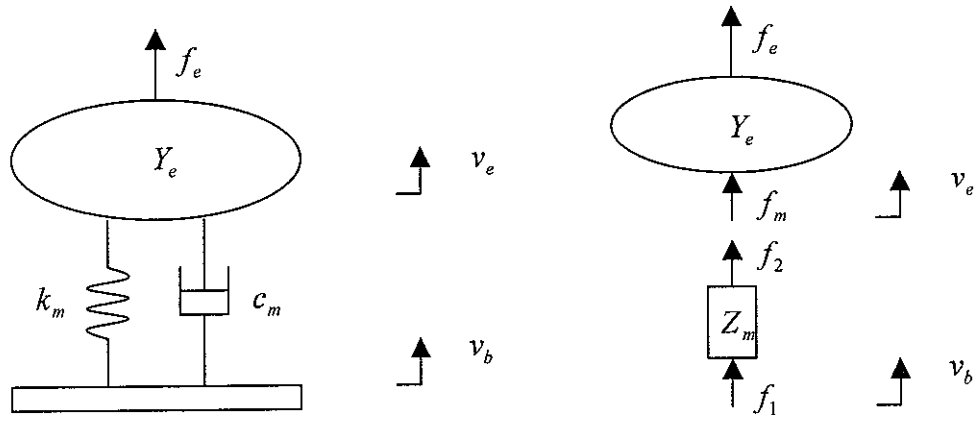

Figure 2.1 Block diagram for a vibrating system with a lumped parameter isolator undergoing harmonic base motion

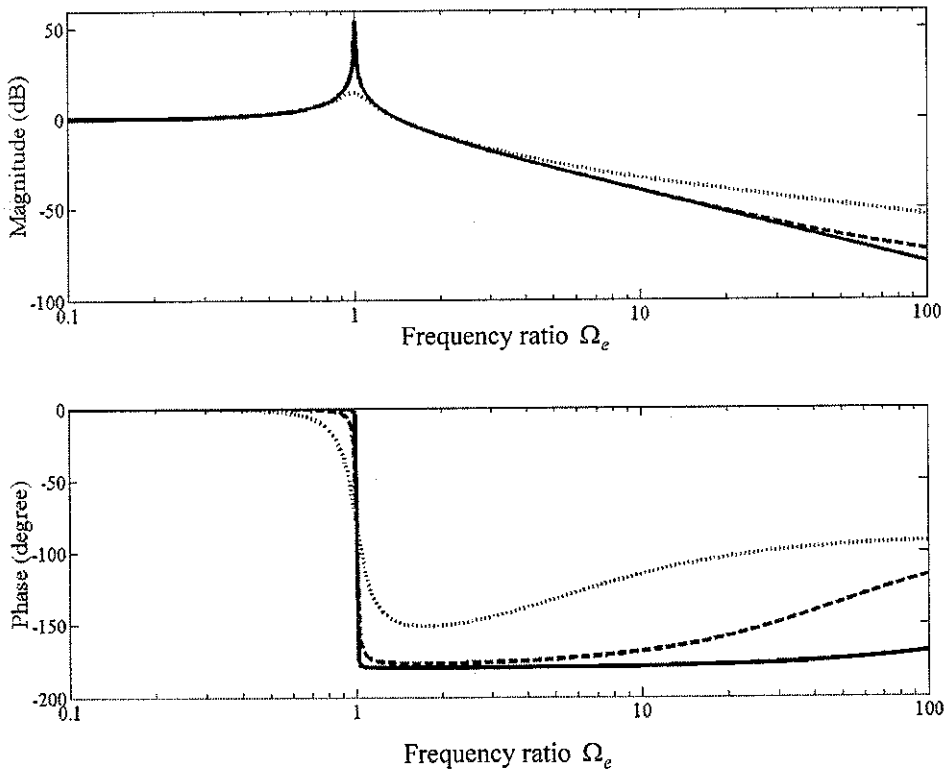

Figure 2.2 Transmissibility of the system with a lumped parameter isolator undergoing harmonic base motion for different values of passive viscous damping in the mount ζ_m =0.001(solid line), 0.01(dashed line), 0.1(dotted line) respectively

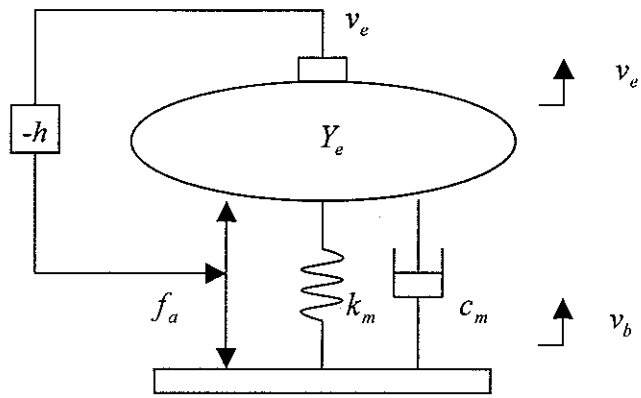

Figure 2.3 Block diagram for the vibrating system with a lumped parameter isolator excited by harmonic base motion under AVF control

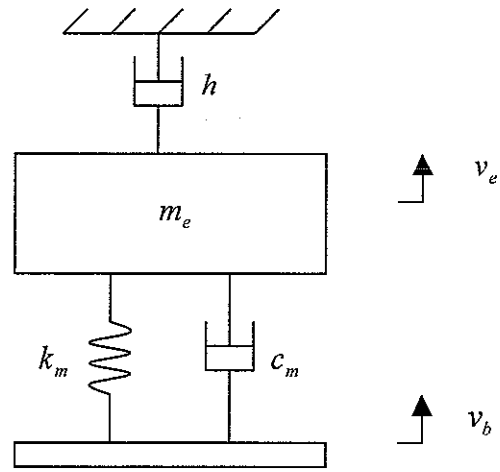

Figure 2.4 Mechanical representation of the absolute velocity feedback control effect as a skyhook damper h

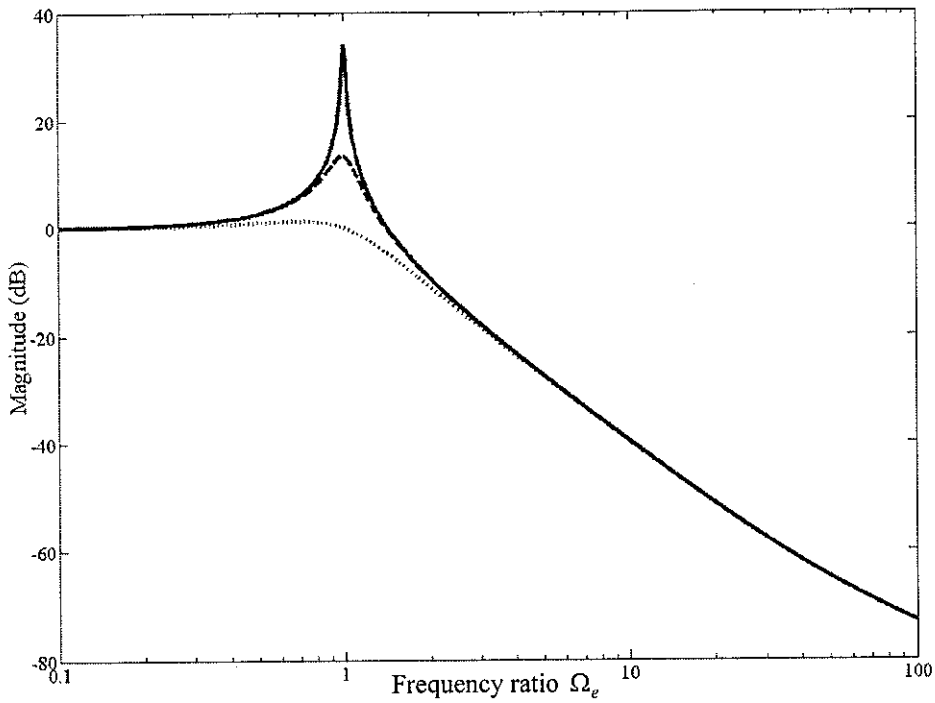

Figure 2.5 Transmissibility of the system with a lumped parameter isolator excited by harmonic base motion under AVF control for a fixed passive damping ratio $\zeta_m = 0.01$ and different values of active damping ratio $\zeta_a = 0$ (solid line), $\zeta_a = 0.1$ (dashed line) and $\zeta_a = 0.5$ (dotted line)

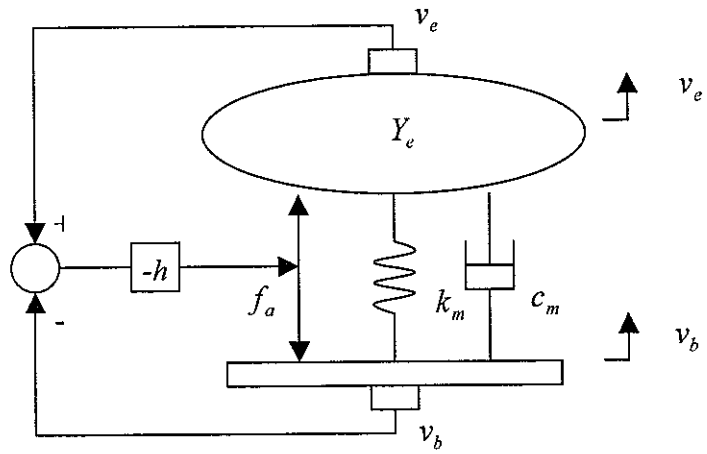

Figure 2.6 Block diagram for the vibrating system with a lumped parameter isolator excited by a base motion under RVF control

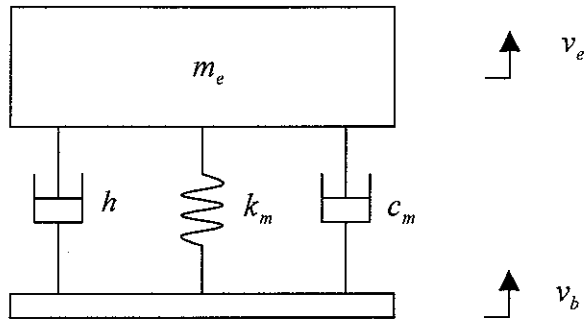

Figure 2.7 Mechanical representation of the relative velocity feedback control effect as an equivalent passive viscous damper h

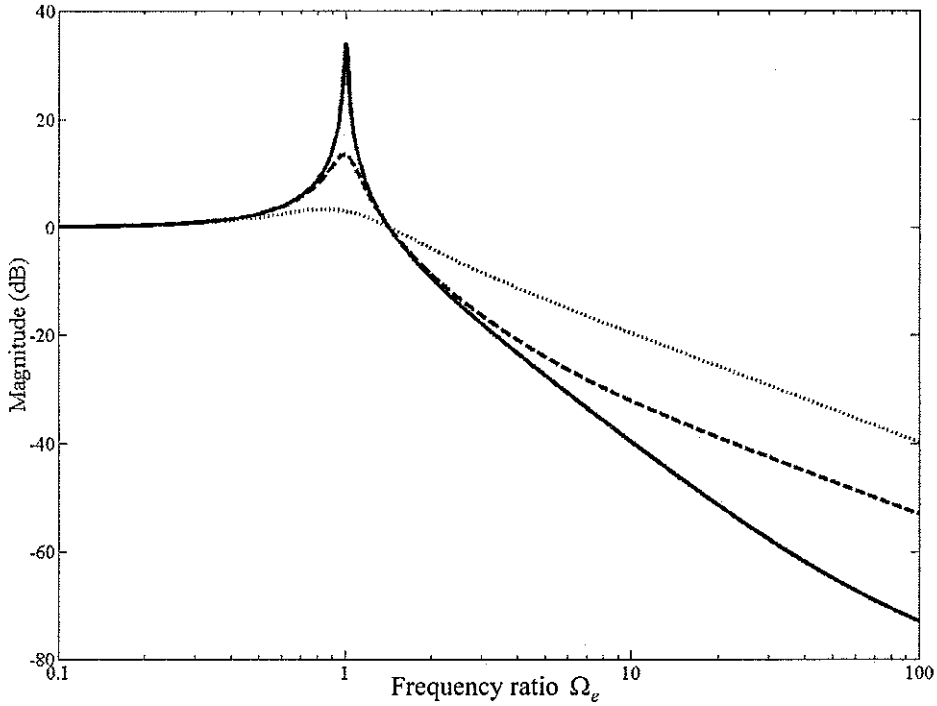

Figure 2.8 Transmissibility of the system with a lumped parameter isolator excited by harmonic base motion under RVF control for a fixed passive damping ratio $\zeta_m = 0.01$ and different values of active damping ratio $\zeta_a = 0$ (solid line), $\zeta_a = 0.1$ (dashed line) and $\zeta_a = 0.5$ (dotted line)

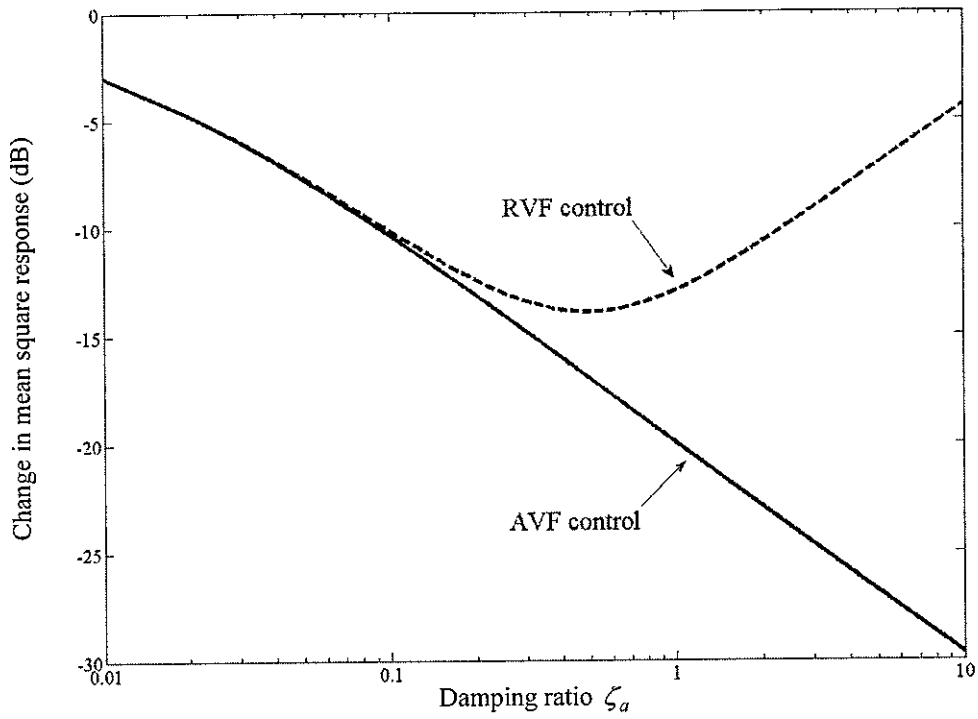

Figure 2.9 Normalised change in mean square displacements for the system with a lumped parameter isolator undergoing harmonic base motion for different control strategies compared to the original passive system when the viscous damping ratio of the mount $\zeta_m = 0.01$

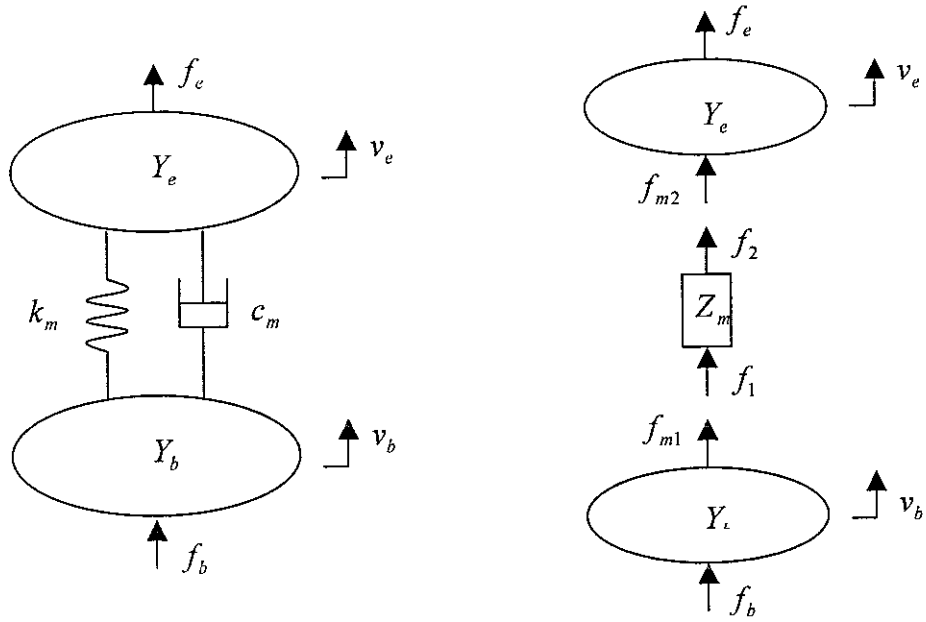

Figure 2.10 Block diagram for the vibrating system with a lumped parameter isolator on a flexible base

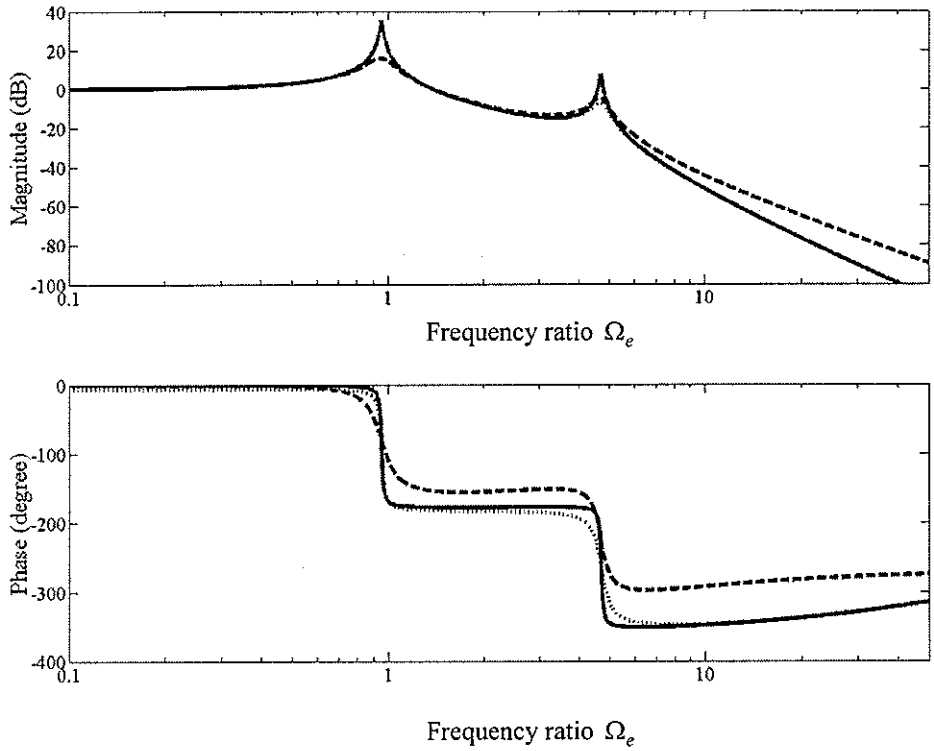

Figure 2.11 Amplitude ratio of the system with a lumped parameter isolator on a flexible base when $\mu_b = 0.5$, $\mu_k = 0.1$ and $\zeta_m = \eta_b = 0.01$ (solid line), $\zeta_m = 0.1$, $\eta_b = 0.01$ (dashed line), $\zeta_m = 0.01$, $\eta_b = 0.1$ (dotted line) respectively

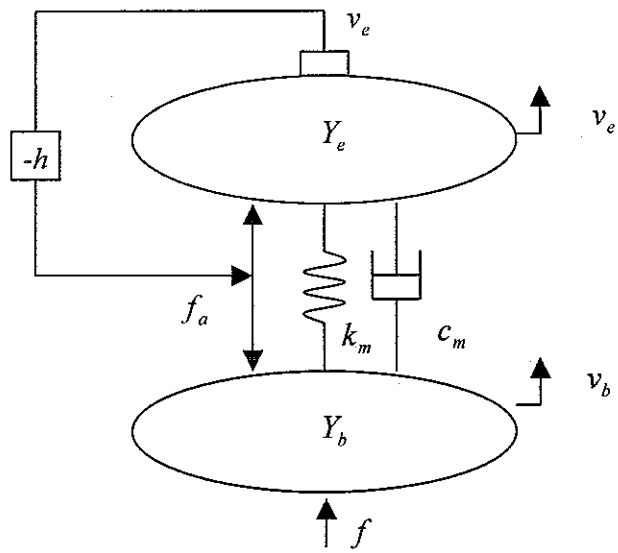

Figure 2.12 Block diagram for the vibrating system with a lumped parameter isolator on a flexible base under AVF control

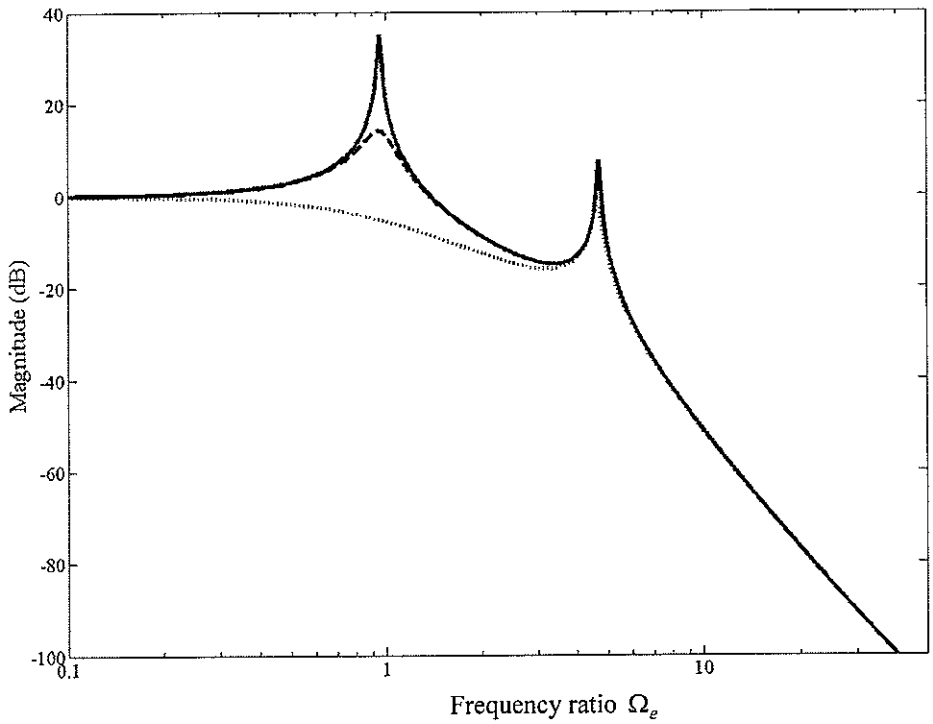

Figure 2.13 Amplitude ratio of the system with a lumped parameter isolator on a flexible base under AVF control when $\mu_b = 0.5$, $\mu_k = 0.1$, $\zeta_m = \eta_b = 0.01$ and $\zeta_a = 0$ (solid line), $\zeta_a = 0.1$ (dashed line) and $\zeta_a = 1$ (dotted line).

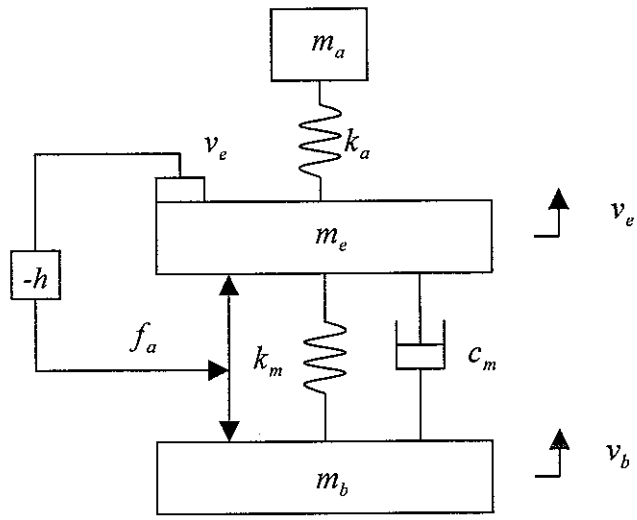

Figure 2.14 An unstable example of the system with a lumped parameter isolator on a flexible base under AVF control

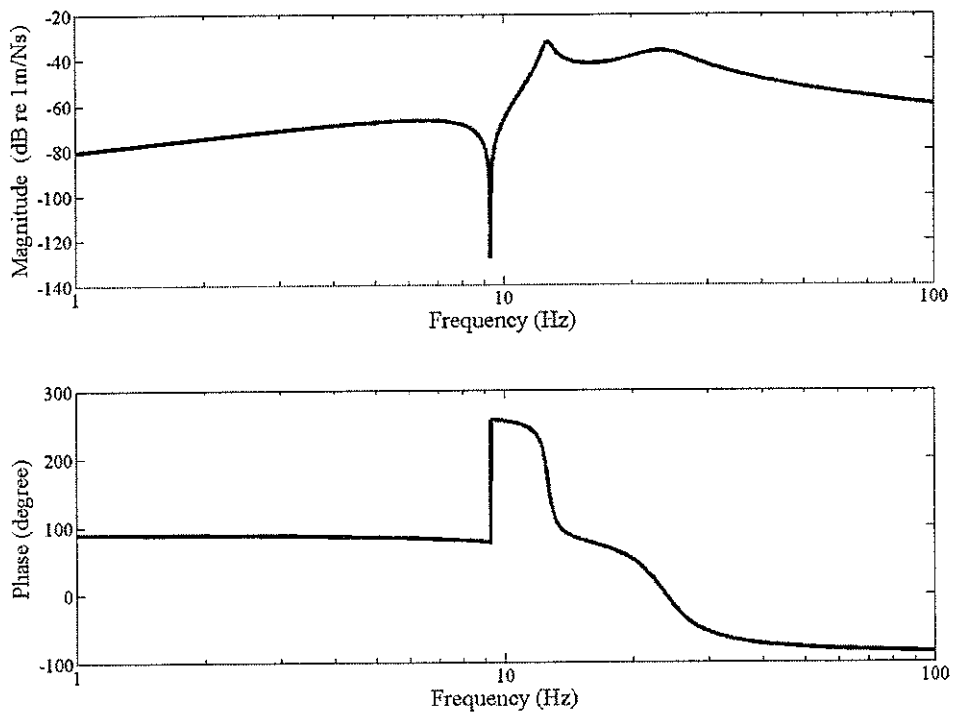

Figure 2.15 Frequency response of the plant response for the unstable case of the system shown in Figure 2.14

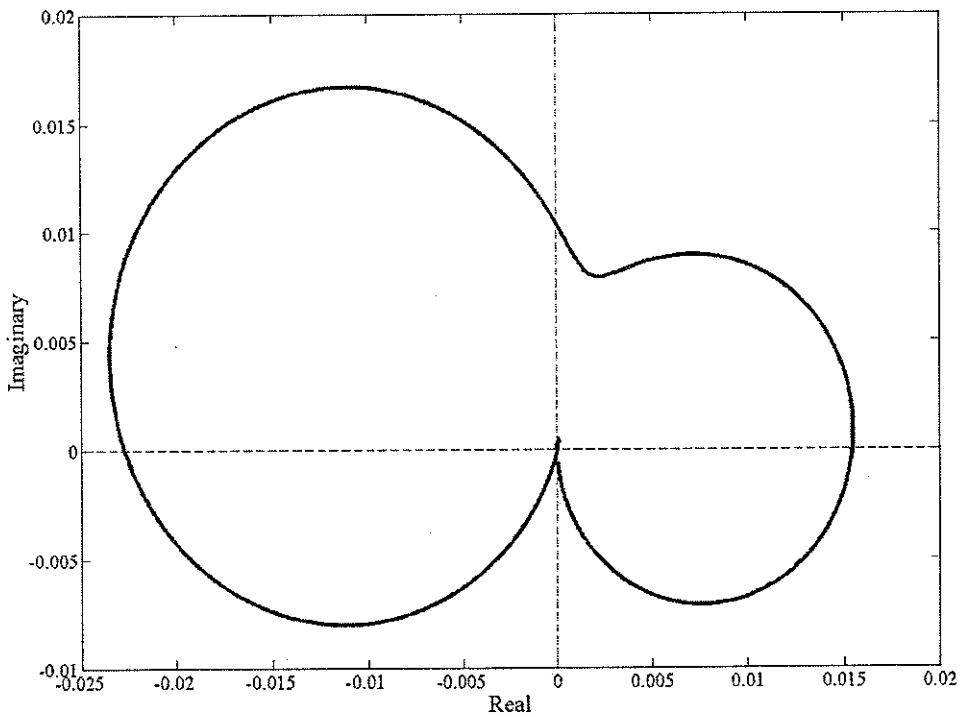

Figure 2.16 Nyquist plot of the plant response for the unstable case of the system shown in Figure 2.14

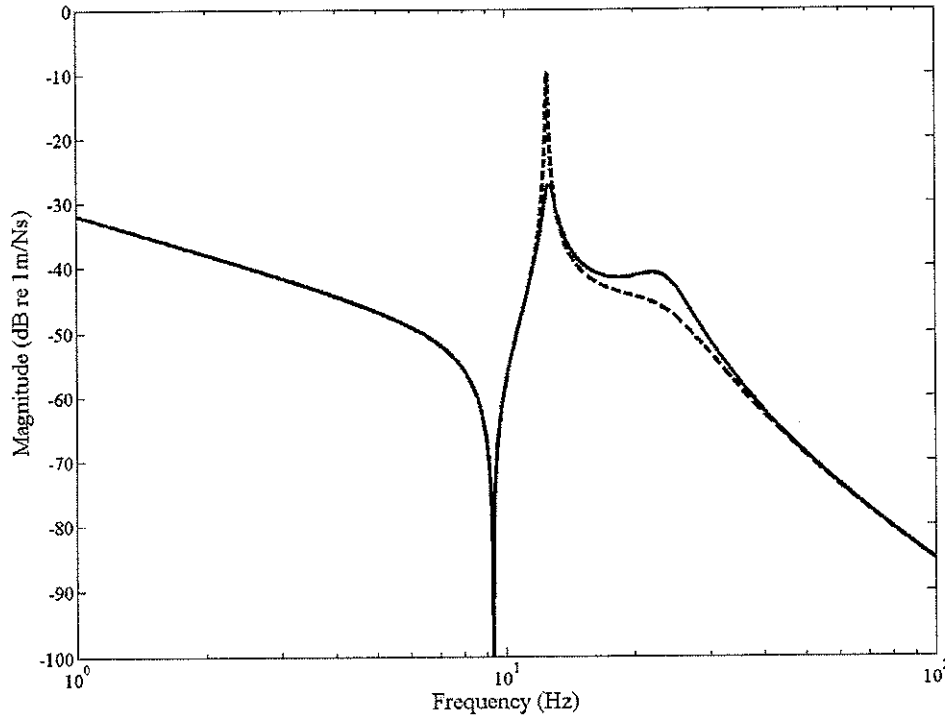

Figure 2.17 Open and closed response from a force on the base structure to the equipment velocity for the unstable case of the system shown in Figure 2.14

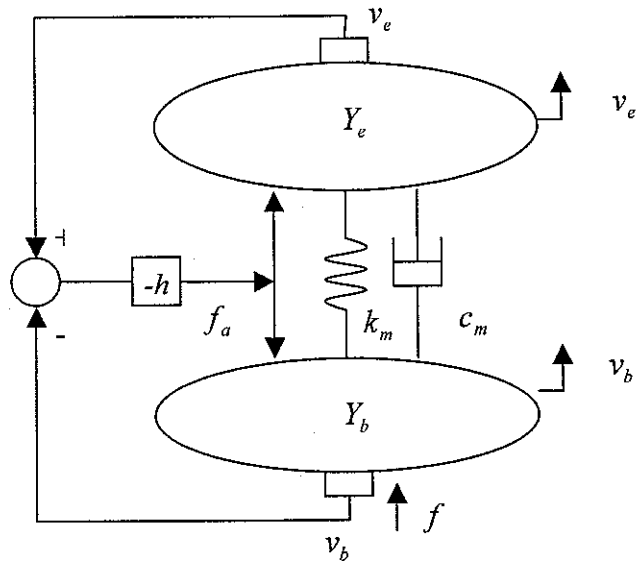

Figure 2.18 Block diagram for the vibrating system with a lumped parameter isolator on a flexible base under RVF control

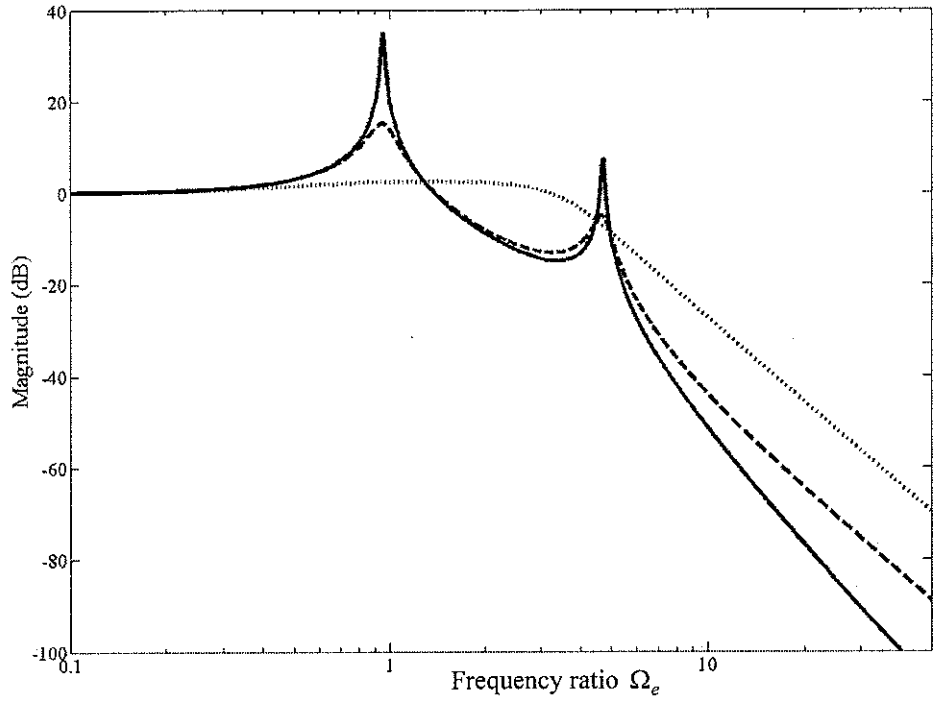

Figure 2.19 Amplitude ratio of the system with a lumped parameter isolator on a flexible base under RVF control when $\mu_b = 0.5$, $\mu_k = 0.1$, $\zeta_m = \eta_b = 0.01$ and $\zeta_a = 0$ (solid line), $\zeta_a = 0.1$ (dashed line) and $\zeta_a = 1$ (dotted line).

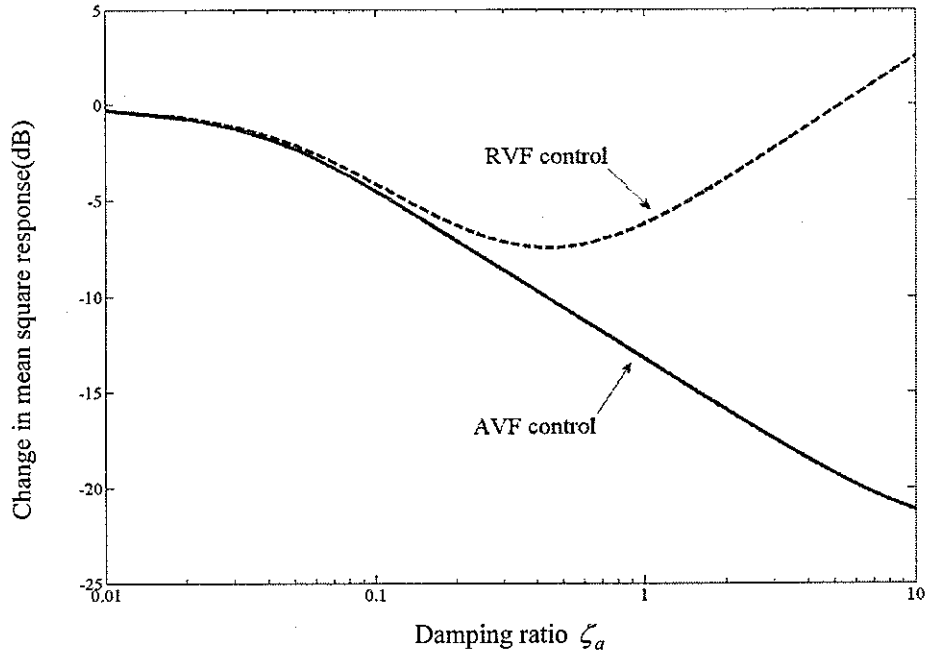

Figure 2.20 Normalised change in mean square displacements for the system with a lumped parameter isolator on a flexible base for different control strategies compared to the original passive system when $\mu_b = 0.5$, $\mu_k = 0.1$, $\zeta_m = \eta_b = 0.01$

3. Vibration isolation systems with a distributed parameter isolator

3.1 Introduction

Vibration isolation systems with a distributed parameter isolator are investigated in this section. The distributed parameter mount is represented by a elastic rod. Absolute velocity feedback control and relative velocity feedback control are applied to such systems. The stability is investigated and control performance is analyzed and compared.

3.2 A vibration isolation system with a distributed parameter mount undergoing harmonic base motion

A vibrating system with a distributed parameter mount undergoing harmonic base motion is analyzed in this section. The mount could be represented by an elastic rod, for example, which itself has distributed mass and stiffness. The frequency response of the system is studied and two different control strategies are applied.

3.2.1 Passive system

A vibrating system with a distributed parameter mount undergoing harmonic base motion is modelled as in Figure 3.1. For convenience the mount is modelled as an elastic rod. For a finite free-free rod, the impedance matrix is given by [13, 14]:

$$\mathbf{Z}_r = \begin{bmatrix} Z_{11} & Z_{12} \\ Z_{21} & Z_{22} \end{bmatrix} = \begin{bmatrix} -jS\sqrt{E^*\rho}\cot(k_l^* L) & j\dfrac{S\sqrt{E^*\rho}}{\sin(k_l^* L)} \\ j\dfrac{S\sqrt{E^*\rho}}{\sin(k_l^* L)} & -jS\sqrt{E^*\rho}\cot(k_l^* L) \end{bmatrix} \tag{3.1}$$

where L, S, E^*, ρ are the length, cross-sectional area, Young's modulus and density of the rod, respectively; to account for damping in the rod, the Young's modulus is assumed to be complex, i.e. $E^* = E(1+j\eta_m)$, where η_m is the loss factor;

$k_l^* \approx k_l(1-j\eta_m/2)$ is the longitudinal wave number, where $k_l = \sqrt{\rho/E}\omega$ is the wavenumber in the undamped rod, and ω is angular frequency.

The equations of motion are

$$\begin{aligned} v_e &= Y_e\left(f_e + f_m\right) \\ f_m &= -f_2 \\ \begin{bmatrix} f_1 \\ f_2 \end{bmatrix} &= \mathbf{Z}_r \cdot \begin{bmatrix} v_b \\ v_e \end{bmatrix} = \begin{bmatrix} Z_{11} & Z_{12} \\ Z_{21} & Z_{22} \end{bmatrix}\begin{bmatrix} v_b \\ v_e \end{bmatrix} \end{aligned} \tag{3.2a,b,c}$$

The velocity of the equipment can be written as

$$v_e = \frac{Y_e}{1+Y_eZ_{22}} f_e - \frac{Y_eZ_{21}}{1+Y_eZ_{22}} v_b \tag{3.3}$$

Without the external force f_e exciting on the equipment, the transmissibility can be written as

$$T = -\frac{Y_eZ_{21}}{1+Y_eZ_{22}} \tag{3.4}$$

If the equipment is modelled as a mass, and the appropriate impedances in equation (3.1) are substituted into equation (3.4), the non-dimensional transmissibility can be written as a function of three parameters namely Ω_e (non-dimensional frequency ratio), μ_m (mass ratio) and η_m (loss factor)

$$T = \frac{1}{\cos\left[\sqrt{\mu_m}\left(1-j\frac{\eta_m}{2}\right)\Omega_e\right] - \frac{\Omega_e}{\sqrt{\mu_m}}\left(1-j\frac{\eta_m}{2}\right)\sin\left[\sqrt{\mu_m}\left(1-j\frac{\eta_m}{2}\right)\Omega_e\right]} \tag{3.5}$$

where $\Omega_e = \omega/\omega_e$, $\omega_e = \sqrt{k_s/m_e}$ and $k_s = ES/L$; $\mu_m = \rho SL/m_e$ is the ratio of the mass of the mount to the mass of the equipment.

Figure 3.2 shows the frequency response of the transmissibility with different loss factors in the isolator. The dashed lines are through the peaks in the transmissibility for different loss factors. These peaks occur due to resonances in the mount, which can be determined by setting $\sin\left(\sqrt{\mu_m}\Omega_e\right) = 0$ and assuming $\eta_m << 1$ in equation (3.5) to give as

$$T = \frac{1}{\cos\left(\sqrt{\mu_m}\Omega_e\right)\cos\left(j\frac{1}{2}\sqrt{\mu_m}\eta_m\Omega_e\right) + \sin\left(\sqrt{\mu_m}\Omega_e\right)\sin\left(j\frac{1}{2}\sqrt{\mu_m}\eta_m\Omega_e\right)} \cdots$$

$$\cdots - \frac{\Omega_e}{\sqrt{\mu_m}}\left(1 - j\frac{\eta_m}{2}\right)\left[\sin\left(\sqrt{\mu_m}\Omega_e\right)\cos\left(j\frac{1}{2}\sqrt{\mu_m}\eta_m\Omega_e\right) + \cos\left(\sqrt{\mu_m}\Omega_e\right)\sin\left(j\frac{1}{2}\sqrt{\mu_m}\eta_m\Omega_e\right)\right] \quad (3.6)$$

Because $\eta_m << 1$, $\sqrt{\mu_m}\eta_m\Omega_e / 2 << 1$ at reasonable frequency region, so that

$$\sin\left(j\frac{1}{2}\sqrt{\mu_m}\eta_m\Omega_e\right) \approx j\frac{1}{2}\sqrt{\mu_m}\eta_m\Omega_e$$
$$\cos\left(j\frac{1}{2}\sqrt{\mu_m}\eta_m\Omega_e\right) \approx 1 \quad (3.7a,b)$$

Substituting them into equation (3.6), the maximum line can be given as

$$|T|_{\max} \approx \frac{2}{\eta_m\Omega_e^2} \quad (3.8)$$

which is a function of the loss factor in the mount and decreases by 40 dB/decade.

The dotted line in Figure 3.2 is the minimum (bottom) line of the transmissibility across the rod. When $\cos\left[\sqrt{\mu_m}\left(1 - j\eta_m / 2\right)\Omega_e\right] = 0$, i.e. the term including $\Omega_e / \sqrt{\mu_m}$ dominates in equation (3.5), the minimum line can be determined to give

$$|T|_{\min} \approx \frac{\sqrt{\mu_m}}{\Omega_e} \quad (3.9)$$

which decreases by 20 dB/decade

The dash-dot line in Figure 3.2 is the transmissibility of the system if the rod is very light compared to the equipment mass, i.e. $\mu_m << 1$, and is given by

$$|T|_{lightrod} \approx \left|\frac{1}{1 - \Omega_e^2}\right| \quad (3.10)$$

The point circled is when equations (3.9) and (3.10) are equal and is given by $\Omega_e \approx 1/\sqrt{\mu_m}$, $|T| \approx \mu_m$. It is only a function of the mass ratio and corresponds to the frequency at which the characteristics of a system with a massless mount and a system with a distributed parameter mount start to deviate.

Thus it can be seen that if the mass of the distributed parameter mount is negligible, the transmissibility tends to roll-off at 40 dB/decade at high frequencies. Due to the effect of the resonances inherent in the mount, the transmissibility at high frequency is

increased compared to the case of the light mount. The lines through the resonance peaks reduce by 40 dB/decade. However, the line through the minima reduces by 20 dB/decade.

3.2.2 The system under Absolute Velocity Feedback control

Figure 3.3 shows the system under absolute velocity feedback control.

- **Control performance**

Substituting f_a for f_e, the equation (3.3) can be rewritten as

$$v_e = \frac{Y_e}{1+Y_e Z_{22}} f_a - \frac{Y_e Z_{21}}{1+Y_e Z_{22}} v_b \tag{3.11}$$

Substituting equation (2.6) into (3.11), the transmissibility under AVF control is given by

$$T = \frac{-Z_{21}}{Z_e + Z_{22} + h} \tag{3.12}$$

If the equipment is modelled as a mass, the transmissibility of the system under AVF control can be written as

$$T = \frac{1}{\cos\left[\sqrt{\mu_m}\left(1-j\frac{\eta_m}{2}\right)\Omega_e\right] - \frac{\Omega_e - j2\zeta_a}{\sqrt{\mu_m}}\left(1-j\frac{\eta_m}{2}\right)\sin\left[\sqrt{\mu_m}\left(1-j\frac{\eta_m}{2}\right)\Omega_e\right]} \tag{3.13}$$

where $\zeta_a = h/2\sqrt{k_s m_e}$ is the damping ratio due to the feedback control.

It can be seen in equation (3.13) that the feedback adds a damping term to the denominator and leaves the numerator unchanged. The action of absolute velocity feedback for such a system is the same as a skyhook damper. Figure 3.4(a) shows the mechanical representation of absolute velocity feedback control on the system with a distributed parameter mount excited by base motion. Figure 3.4(b) depicts the system in terms of a mobility diagram where it is clear that the skyhook damper is effectively in parallel with the equipment mass so that the combined impedance is $Z_t = c_a + j\omega m_e$. Thus, the damping term dominates at low frequencies while the mass term dominates at high frequencies. This explains why in Figure 3.5, which shows the transmissibility for different values of active damping ratio, the resonance peak at fundamental natural frequency of the mounted equipment is suppressed for a high

active damping ratio without amplification at high frequencies. However, there is very little reduction in the resonance peaks due to the distributed parameter mount, especially at frequencies well above the fundamental natural frequency. In the case of a small equipment mass, the AVF control will have better control performance at relatively high resonance frequencies compared to the case of a large equipment mass.

- **Stability analysis**

For the vibrating system with a distributed parameter mount under AVF control shown in Figure 3.3, the plant response from actuator force to absolute equipment velocity is given by

$$G = \frac{Y_e}{1 + Y_e Z_{22}} = \frac{1}{Z_e + Z_{22}} \tag{3.14}$$

Because Z_e and Z_{22} are both point impedances, their phase is between -90° and 90°. Therefore the phase of the plant response G is given by $-90^0 < \angle G < 90^0$, so based on the Nyquist criterion, the system is unconditionally stable.

3.2.3 The system under Relative Velocity Feedback control

Figure 3.6 shows the system under relative velocity feedback control.

- **Control performance**

Substituting (2.12) into equation (3.11), the equipment velocity under RVF control is given by

$$T = \frac{-Z_{21} + h}{Z_e + Z_{22} + h} \tag{3.15}$$

If the equipment has a mass-like mobility, the non-dimensional transmissibility under RVF control can be written as

$$T = \frac{1 + j\frac{2\zeta_a}{\sqrt{\mu_m}}\left(1 - j\frac{\eta_m}{2}\right)\sin\left[\sqrt{\mu_m}\left(1 - j\frac{\eta_m}{2}\right)\Omega_e\right]}{\cos\left[\sqrt{\mu_m}\left(1 - j\frac{\eta_m}{2}\right)\Omega_e\right] - \frac{(\Omega_e - j2\zeta_a)}{\sqrt{\mu_m}}\left(1 - j\frac{\eta_m}{2}\right)\sin\left[\sqrt{\mu_m}\left(1 - j\frac{\eta_m}{2}\right)\Omega_e\right]} \tag{3.16}$$

It can be seen in equation (3.16) that a damping term is added to both the denominator and the numerator. The action of relative velocity feedback is the same as a passive viscous damper acting between the equipment and the base. Figure 3.7 shows the

transmissibility of the system under RVF control for different values of active damping ratio. The resonance peak at the fundamental natural frequency of the mounted equipment and also some resonance peaks due to the distributed parameter mount are attenuated with high active damping ratios, which may not be seen clearly in Figure 3.7 because the attenuation is very small. This is a marginal advantage of RVF compared to AVF. However, the transmissibility away from resonances is amplified at high frequencies so that the overall control performance is worse than that under AVF control. The same to the description in section 2.2.3, Figure 3.8 depicts the change in the mean square velocity compared to the original passive case. At high active damping ratios, the AVF control provides increasing reduction in the mean square response. The performance of the RVF control system is always worse than the performance of the AVF control system and does not produce monotonically reducing mean square response for an increase in active damping ratio.

- **Stability analysis**

The plant response of the system is given by

$$G = \frac{1}{Z_e + Z_{22}} \tag{3.17}$$

which is the same as that for a system under AVF. Therefore, its phase shift ranges between -90° and 90° so that the system is unconditionally stable.

3.2.4 Conclusions

The action of absolute velocity feedback on a system with a distributed parameter mount undergoing harmonic base motion is the same as a skyhook damper, which is unconditionally stable. However the resonance peaks inherent in the mount are suppressed much less than the reduction of the resonance peak at the fundamental natural frequency of the mounted equipment with an increase in the active damping ratio, which is due to the effect of equipment mass.

The action of relative velocity feedback on such a system is the same as a passive viscous damper acting between the equipment and the base, which is also unconditionally stable. The resonance peak at the fundamental natural frequency of the mounted equipment and also some resonance peaks inherent in the mount are attenuated at high active damping ratio, which is the advantage of RVF compared to

AVF. However, the transmissibility is amplified at high frequencies so that the overall control performance is worse than that under AVF control.

3.3 A vibration isolation system with a distributed parameter mount on a flexible base

A vibrating system with a distributed parameter mount on a flexible base is analyzed in this section. The frequency response of the system is studied and two different control strategies are applied.

3.3.1 Passive system

A vibrating system with a distributed parameter mount on a flexible base is modelled as in Figure 3.9. The equations of motion are given by

$$\begin{aligned} v_e &= Y_e\left(f_e + f_{m2}\right) \\ v_b &= Y_b\left(f_b + f_{m1}\right) \\ \begin{bmatrix} f_{m1} \\ f_{m2} \end{bmatrix} &= -\begin{bmatrix} f_1 \\ f_2 \end{bmatrix} = -\begin{bmatrix} Z_{11} & Z_{12} \\ Z_{21} & Z_{22} \end{bmatrix}\begin{bmatrix} v_b \\ v_e \end{bmatrix} \end{aligned} \tag{3.17a,b,c}$$

The velocity of the equipment can be written as

$$v_e = Y_{ee} f_e + Y_{eb} f_b \tag{3.19}$$

where

$$Y_{ee} = \frac{Y_e\left(1+Y_b Z_{11}\right)}{\left(1+Y_e Z_{22}\right)\left(1+Y_b Z_{11}\right) - Y_e Y_b Z_{12} Z_{21}} \tag{3.20}$$

$$Y_{eb} = \frac{-Y_e Y_b Z_{21}}{\left(1+Y_e Z_{22}\right)\left(1+Y_b Z_{11}\right) - Y_e Y_b Z_{12} Z_{21}} \tag{3.21}$$

If the system is only excited by the external force on the base, $f_b = f$, i.e. external force $f_e = 0$, the velocity of the equipment is given by

$$\frac{v_e}{f} = Y_{eb} = \frac{-Y_e Y_b Z_{21}}{\left(1+Y_e Z_{22}\right)\left(1+Y_b Z_{11}\right) - Y_e Y_b Z_{12} Z_{21}} \tag{3.22}$$

If the equipment has a mass-like mobility, and the base structure is modelled as a mass m_b on a complex spring, i.e. $k_b^* = k_b(1+j\eta_b)$, where η_b is the loss factor, the non-dimensional amplitude ratio can be written as

$$\frac{x}{\delta_{st}} = \frac{1}{\left[(1+j\eta_b)-\left(1+\frac{1}{\mu_b}\right)\frac{\Omega_e^2}{\Gamma_b^2}\right]\cos\left[\sqrt{\mu_m}\left(1-j\frac{\eta_m}{2}\right)\Omega_e\right]\cdots}$$

$$\cdots\overline{+\left[\frac{\Omega_e^2}{\Gamma_b^2}-(1+j\eta_b)-\mu_k\mu_m(1+j\eta_m)\right]\frac{\Omega_e}{\sqrt{\mu_m}}\left(1-j\frac{\eta_m}{2}\right)\sin\left[\sqrt{\mu_m}\left(1-j\frac{\eta_m}{2}\right)\Omega_e\right]} \quad (3.23)$$

where $\Gamma_b = \omega_b / \omega_e = 1/\sqrt{\mu_k\mu_b}$ is the natural frequency ratio, $\mu_k = k_s / k_b$ is the stiffness ratio.

Figure 3.10 shows the amplitude ratio of the system with different values of the passive loss factors. It can be seen that the damping in the base structure is only beneficial to the reduction of the peak due to the base dynamics, which is the second peak in Figure 3.10. However, the damping in the distributed parameter mount is effective in reducing all the other resonance peaks.

Figure 3.11 shows the amplitude ratio of the system with different values of natural frequency ratio Γ_b. It can be observed that, with the increase of the natural frequency ratio Γ_b, the reduction rate of the amplitude ratio is increased at high frequencies. When Γ_b tends to be infinity, i.e. the base is fixed, and providing $\eta_b << 1$, the amplitude ratio of the system can be written as

$$T \approx \frac{1}{\cos\left[\sqrt{\mu_m}\left(1-j\frac{\eta_m}{2}\right)\Omega_e\right]-\frac{\Omega_e}{\sqrt{\mu_m}}\left(1-j\frac{\eta_m}{2}\right)\sin\left[\sqrt{\mu_m}\left(1-j\frac{\eta_m}{2}\right)\Omega_e\right]} \quad (3.24)$$

This equation is identical with the transmissibility of the system with a distributed parameter mount undergoing harmonic base motion (equation 3.5).

3.3.2 The system under Absolute Velocity Feedback control

Figure 3.12 shows the system under absolute velocity feedback control.

- **Control performance**

Referring to the description in section 2.2.1, the external force and active forces acting on the base and equipment respectively are given as

$$f_e = f_a \tag{3.25}$$

$$f_b = f - f_a \tag{3.26}$$

Substituting them into equation (3.19),

$$v_e = \left(Y_{ee} - Y_{eb}\right) f_a + Y_{eb} f \tag{3.27}$$

Substituting equation (2.6) into (3.27), the equipment velocity under AVF control can be written as

$$\frac{v_e}{f} = \frac{Y_{eb}}{1 + h\left(Y_{ee} - Y_{eb}\right)} \tag{3.28}$$

where Y_{ee} and Y_{eb} are defined in equation (3.20) and (3.21).

If the equipment has a mass-like mobility, and the base structure is modelled as a mass m_b on a complex spring, the amplitude ratio of the system under AVF control is given by

$$\frac{x}{\delta_{st}} = \frac{1}{\left[\left(1+j\eta_b\right) - \left(1+\frac{1}{\mu_b}\right)\frac{\Omega_e^2}{\Gamma_b^2}\right]\cos\left[\sqrt{\mu_m}\left(1-j\frac{\eta_m}{2}\right)\Omega_e\right] \cdots}$$

$$\cdots + \left[\frac{\Omega_e^2}{\Gamma_b^2} - \left(1+j\eta_b\right) - \mu_k\mu_m\left(1+j\eta_m\right)\right]\frac{\Omega_e}{\sqrt{\mu_m}}\left(1-j\frac{\eta_m}{2}\right)\sin\left[\sqrt{\mu_m}\left(1-j\frac{\eta_m}{2}\right)\Omega_e\right] \cdots$$

$$\cdots + j2\zeta_a\left\{\mu_k\Omega_e\left[\cos\left(\sqrt{\mu_m}\left(1-j\frac{\eta_m}{2}\right)\Omega_e\right) - 1\right] + \frac{1}{\sqrt{\mu_m}}\left(1-j\frac{1}{2}\eta_m\right)\left(1+j\eta_b - \frac{\Omega_e^2}{\Gamma_b^2}\right)\sin\left(\sqrt{\mu_m}\left(1-j\frac{\eta_m}{2}\right)\Omega_e\right)\right\} \tag{3.29}$$

The feedback adds a damping term to the denominator and leaves the numerator unchanged. Figure 3.13 shows the amplitude ratio for the system under AVF control with different values of the active damping ratio ζ_a. The resonance peak at the fundamental natural frequency of the mounted equipment is attenuated with an increase in the damping ratio. The resonance peak at the natural frequency of the base, which is the second peak in Figure 3.13, is also attenuated for high damping ratios. However, the resonance peaks due to the mount are reduced much less, especially at relatively high frequencies above the fundamental natural frequency as discussed in section 3.1.2. Also it should be noted that some resonance peaks inherent in the

distributed parameter mount, such as the third peak in Figure 3.13, are amplified under AVF control which might cause instability.

- **Stability analysis**

The plant response from actuator force to absolute equipment velocity for this system under AVF control is given by

$$G = Y_{ee} - Y_{eb} \tag{3.30}$$

where Y_{ee} is the response of the equipment per unit actuator force applied directly on the equipment and Y_{eb} is the response of the equipment per unit actuator force applied on the base. Because Y_{ee} is a point mobility, it has a phase between -90° and 90°. It is a stable part because it is only in the right half in the complex plane. However, Y_{eb} is a transfer mobility, which could be in either left or right half in the complex plane. So it is a potential threat to instability of the control system. Moreover, if the control system is unstable, there is at least one loop in the left half in the Nyquist plot of the plant response which encloses the unstable point (-1, 0j). For the system analyzed here, only at resonance frequencies can phase of the plant response generate such loops, and hence create an unstable system. So if at some resonance frequencies where the transfer mobility is greater than the point mobility, the control system has the potential to become unstable at high control gains.

For a multi-degree-of freedom system, the mobility can be written as [2]

$$Y = \frac{v_r}{f_s} = \sum_{j=1}^{\infty} \frac{j\omega \cdot \phi_r^{(j)} \cdot \phi_s^{(j)}}{K_j \left(1 - \Omega_j^2 + j2\zeta_j \Omega_j\right)} \tag{3.31}$$

where $\phi_r^{(j)}$ and $\phi_s^{(j)}$ are respectively the j^{th} mode shape evaluated at the response point r and excitation point s; K_j, M_j and ζ_j are modal stiffness, modal mass and modal damping ratio of the j^{th} mode with corresponding natural frequency $\omega_j = \sqrt{K_j / M_j}$; $\Omega_j = \omega / \omega_j$ is the non-dimensional frequency.

At a resonance frequency, in a lightly damped system, when only one mode dominates the response, the point and transfer mobility for the system can be written as

$$Y_{ee} \approx \frac{j\omega\left[\phi_{\mathrm{e}}^{(j)}\right]^2}{j2K_j\zeta_j\Omega_j} \tag{3.32}$$

$$Y_{eb} \approx \frac{j\omega\left(\phi_{\mathrm{b}}^{(j)}\phi_{\mathrm{e}}^{(j)}\right)}{j2K_j\zeta_j\Omega_j} \tag{3.33}$$

So that the plant response is given by

$$G = Y_{ee} - Y_{eb} \approx \frac{j\omega\left[\phi_{\mathrm{e}}^{(j)}\right]^2\left(1-\frac{\phi_{\mathrm{b}}^{(j)}}{\phi_{\mathrm{e}}^{(j)}}\right)}{j2K_j\zeta_j\Omega_j} \tag{3.34}$$

where $\phi_{\mathrm{e}}^{(j)}$ and $\phi_{\mathrm{b}}^{(j)}$ are the j^{th} mode shape evaluated at the equipment and base respectively.

Based on the Nyquist criterion, for instability, one requires at a resonant frequency

$$\frac{\phi_{\mathrm{b}}^{(j)}}{\phi_{\mathrm{e}}^{(j)}} > 1 \tag{3.35}$$

i.e. $\left|\phi_{\mathrm{b}}^{(j)}\right| > \left|\phi_{\mathrm{e}}^{(j)}\right|$ and mode shapes of the system evaluated at the equipment and base need to have the same sign.

Figure 3.14 and 3.15 are respectively the frequency response and Nyquist plot of the plant response for a potentially unstable system. It is clear in Figure 3.14 that the phase shift around 12.7 Hz generates a loop on the left half of the complex plane that crosses the negative real axis, which causes the system to be potentially unstable at high control gains.

An increase in the system damping is beneficial in stabilizing the control system by reducing the phase around the resonance frequencies. Figure 3.16 shows the frequency response of the plant response for a potentially unstable system with different values of loss factor in the mount. It can be noted that the phase at the resonance of 12.7 Hz is suppressed for a high loss factor so that the system becomes stable. So the situation of having a lightly damped system, i.e. one mode dominating the response at resonance frequencies, is the worst case for instability.

Therefore, equation (3.35) provides a simple method to determine the stability of the system in terms of the mode shapes of the system. According to the definition of mode shapes $\phi_e^{(j)}$ and $\phi_b^{(j)}$, this instability condition means that the displacement of the base is greater than the displacement of the equipment and these two displacements are in phase at the j^{th} natural frequency.

At the j^{th} natural frequency, i.e. $\Omega_j = 1$, equation (3.34) can be rewritten as

$$G = \frac{\left[\phi_e^{(j)}\right]^2 \left(1 - \frac{\phi_b^{(j)}}{\phi_e^{(j)}}\right)}{2\sqrt{K_j M_j}\zeta_j} \tag{3.36}$$

In case of $\phi_b^{(j)} / \phi_e^{(j)} > 1$, i.e. the system has the potential to become unstable, with constant control gain h, the open loop response is given by

$$hG = h\frac{\left[\phi_e^{(j)}\right]^2 \left(1 - \frac{\phi_b^{(j)}}{\phi_e^{(j)}}\right)}{2\sqrt{K_j M_j}\zeta_j} \tag{3.37}$$

To guarantee stability, the quantity in equation (3.37) must be greater than -1, so that the maximum gain h_{max} that can be applied to the system is

$$h_{max} = \frac{2\sqrt{K_j M_j}\zeta_j}{\left[\phi_e^{(j)}\right]^2 \left(\frac{\phi_b^{(j)}}{\phi_e^{(j)}} - 1\right)} \tag{3.38}$$

This instability condition in terms of the mode shapes can also be applied to the system with a lumped parameter isolator on a flexible base. For the system shown in Figure 2.14, when $\omega_j = 23.7$ Hz, the relative displacements in the mode shape evaluated at the equipment and base is given by $\begin{bmatrix}\phi_e & \phi_b\end{bmatrix}^T = \begin{bmatrix}0.59 & -0.57\end{bmatrix}^T$. The instability condition given by equation (3.35) is not satisfied, so the system is stable. When $\omega_j = 12.6$ Hz, the corresponding mode shape relative displacements is $\begin{bmatrix}\phi_e & \phi_b\end{bmatrix}^T = \begin{bmatrix}0.28 & 0.65\end{bmatrix}^T$. The instability condition is satisfied so the system becomes potentially unstable. The same result is achieved as seen in Figure 2.17 by the three instability conditions generalized by Elliott et al [9].

3.3.3 The system under Relative Velocity Feedback control

Figure 3.17 shows the system under relative velocity feedback control.

- **Control performance**

Substituting equation (2.12) into (3.27), and because

$$v_b = (Y_{eb} - Y_{bb}) f_a + Y_{bb} f \tag{3.39}$$

The equipment velocity under RVF control is given by

$$\frac{v_e}{f} = \frac{Y_{eb} + h(Y_{ee}Y_{bb} - Y_{eb}{}^2)}{1 + h(Y_{ee} + Y_{bb} - 2 \cdot Y_{eb})} \tag{3.40}$$

where Y_{bb} is the input mobility of the base when coupled to the rest of the system, and is given by

$$Y_{bb} = \frac{Y_b(1 + Y_e Z_{22})}{(1 + Y_e Z_{22})(1 + Y_b Z_{11}) - Y_e Y_b Z_{12} Z_{21}} \tag{3.41}$$

If the equipment has a mass-like mobility, and the base structure is modelled as a mass on a complex spring, the amplitude ratio is given by

$$\frac{x}{\delta_{st}} = \frac{1 + j\zeta_a \frac{2}{\sqrt{\mu_m}}\left(1 - j\frac{\eta_m}{2}\right)\sin\left[\sqrt{\mu_m}\left(1 - j\frac{\eta_m}{2}\right)\Omega_e\right]}{\left[(1 + j\eta_b) - \left(1 + \frac{1}{\mu_b}\right)\frac{\Omega_e^2}{\Gamma_b^2}\right]\cos\left[\sqrt{\mu_m}\left(1 - j\frac{\eta_m}{2}\right)\Omega_e\right]} \cdots$$

$$\cdots + \left[\frac{\Omega_e^2}{\Gamma_b^2} - (1 + j\eta_b) - \mu_k\mu_m(1 + j\eta_m)\right]\frac{\Omega_e}{\sqrt{\mu_m}}\left(1 - j\frac{\eta_m}{2}\right)\sin\left[\sqrt{\mu_m}\left(1 - j\frac{\eta_m}{2}\right)\Omega_e\right] \cdots$$

$$\cdots + j2\zeta_a\left\{2\mu_k\Omega_e\left[\cos\left(\sqrt{\mu_m}\left(1 - j\frac{\eta_m}{2}\right)\Omega_e\right) - 1\right] + \frac{(1 - j\eta_m/2)}{\sqrt{\mu_m}}\left[1 + j\eta_b - \left(1 + \frac{1}{\mu_b}\right)\frac{\Omega_e^2}{\Gamma_b^2}\right]\sin\left(\sqrt{\mu_m}\left(1 - j\frac{\eta_m}{2}\right)\Omega_e\right)\right\} \tag{3.42}$$

In this case, the feedback system adds a damping term both to the denominator and the numerator. Figure 3.18 shows the amplitude ratio for the system under RVF control with different values of the active damping ratio ζ_a. The resonance peak at the fundamental natural frequency of the mounted equipment and some resonance peaks due to the distributed parameter mount are attenuated with high damping ratio ζ_a, while the amplitude ratio is amplified at high frequencies well above the fundamental natural frequency. Therefore the overall control performance under RVF is worse than

that under AVF. The same to the description in section 2.3.3, Figure 3.19(a) depicts the change in normalised mean square displacements compared to the original passive system when the system under AVF control is stable. In contrast, Figure 3.19(b) depicts the change in normalised mean square displacements when the system under AVF control has potential to be unstable. Instability of the AVF control is seen to occur when the active damping ratio is increased.

- **Stability analysis**

In this case the control law is designed such that energy can only be extracted from the mechanical structure. The control system is thus unconditionally stable, and also said to be dissipative [15].

The time averaged power generated by the control force for the system under RVF control at any particular frequency can be written as [2]

$$P_{f_a} = \frac{1}{2}\mathrm{Re}\left\{f_a \cdot v_e^*\right\} + \frac{1}{2}\mathrm{Re}\left\{-f_a \cdot v_b^*\right\} \tag{3.43}$$

Substituting $f_a = -h\left(v_e - v_b\right)$ into the equation above so that

$$P_{f_a} = -\frac{1}{2}h\left|v_e - v_b\right|^2 \tag{3.44}$$

Therefore, the power generated by the control force is always negative. That means the control system only extracts energy from the mechanical system so that such a system under RVF control is unconditionally stable.

The mode shape method can also be applied to this RVF control system. For the system under RVF control, the plant response from the actuator force to the difference between absolute equipment velocity and absolute base velocity is given by

$$G = Y_{ee} + Y_{bb} - 2Y_{eb} \tag{3.45}$$

At a resonance frequency, in a lightly damped system, when only one mode dominates the response, the plant response can be written as

$$G = Y_{ee} + Y_{bb} - 2Y_{eb} \approx \frac{j\omega\left[\phi_e^{(j)} - \phi_b^{(j)}\right]^2}{j2K_j\zeta_j\Omega_j} \tag{3.46}$$

which is always nonnegative. Therefore, the plant response under RVF control is always in the right half in the complex plane and the system is therefore unconditionally stable.

3.3.4 Conclusions

The action of absolute velocity feedback on a system with a distributed parameter mount on a flexible base is similar to a skyhook damper. The resonance peak at the fundamental natural frequency of the mounted equipment is attenuated with an increase in the active damping ratio. The resonance peak at the natural frequency of the base is also attenuated at high damping ratios. However, the resonance peaks due to the mount are reduced much less, especially at relatively high frequencies above the fundamental natural frequency due to the effect of equipment mass. Also the descending rate of the amplitude ratio of the system is affected by the natural frequency ratio Γ_b. Moreover, such a control system is only conditionally stable. A simple method to determine the stability of the system in terms of the mode shapes of the system has been developed. The maximum control gain and the effect of damping to the stability are also discussed.

The action of relative velocity feedback on such a system is the same as a passive viscous damper, which is unconditionally stable. The resonance peak at the fundamental natural frequency of the mounted equipment and some resonance peaks due to the distributed parameter mount are attenuated with high active damping ratio ζ_a, while the amplitude ratio is amplified at high frequencies well above the fundamental natural frequency. Therefore its control performance is worse than that of the system under AVF control, especially at high active damping ratios.

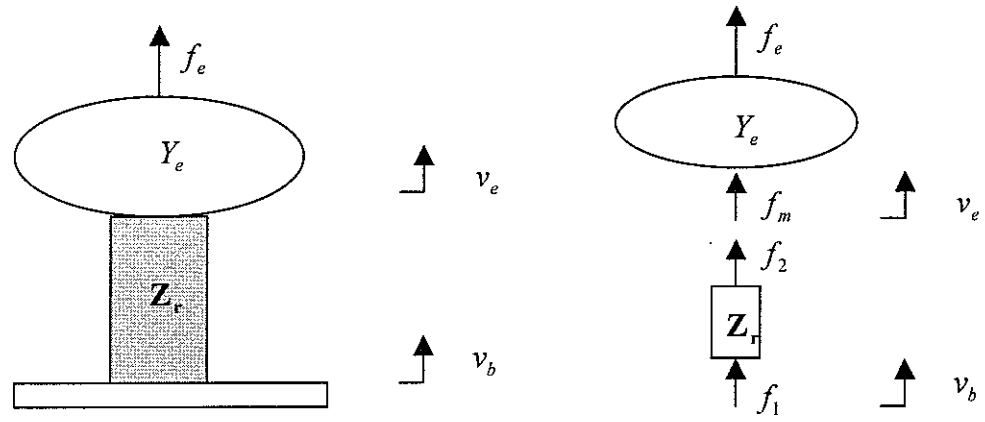

Figure 3.1 Block diagram for the vibrating system with a distributed parameter mount undergoing harmonic base motion

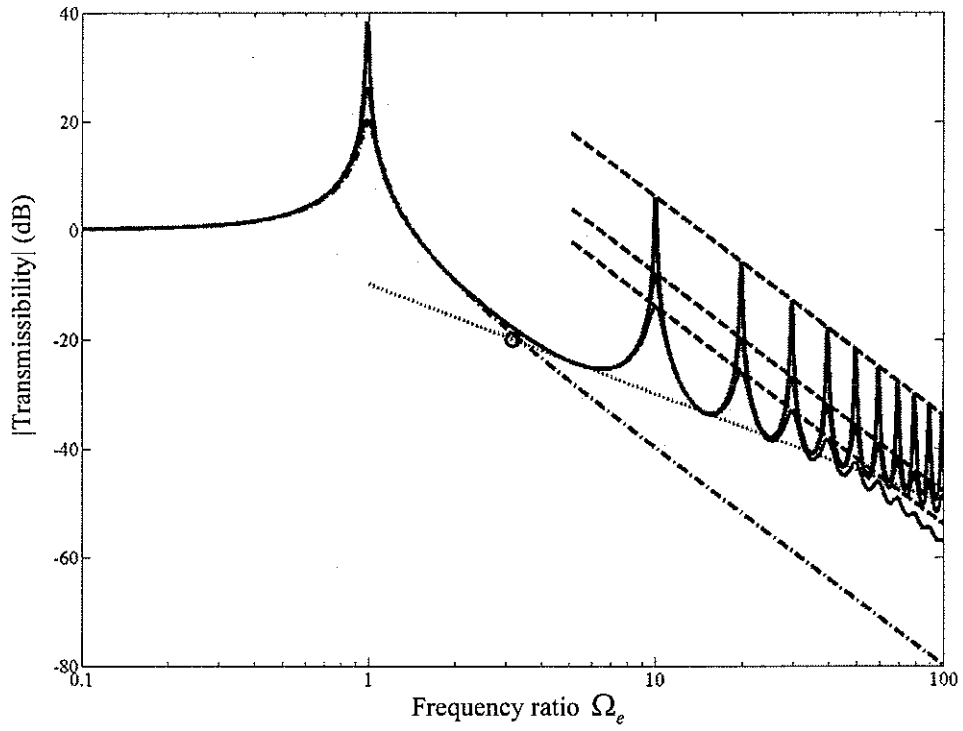

Figure 3.2 Transmissibility of the system in Figure 3.1 when $\mu_m = 0.1$; the loss factor is $\eta_m = 0.01$, 0.05, and 0.1 respectively. The dashed lines pass through the rod resonant peaks. The dotted line passes through the minima of the transmissibility. The dash-dot line is for the light rod isolator. The point cycled is the intersection of the transmissibility of the system with massless isolator and with distributed parameter isolator.

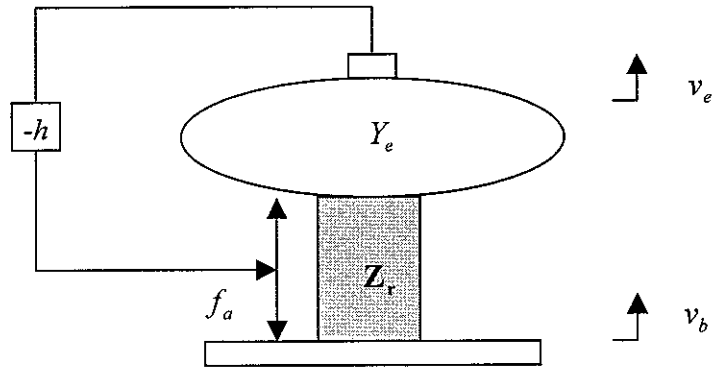

Figure 3.3 Block diagram for the vibrating system with a distributed parameter mount excited by harmonic base motion under AVF control

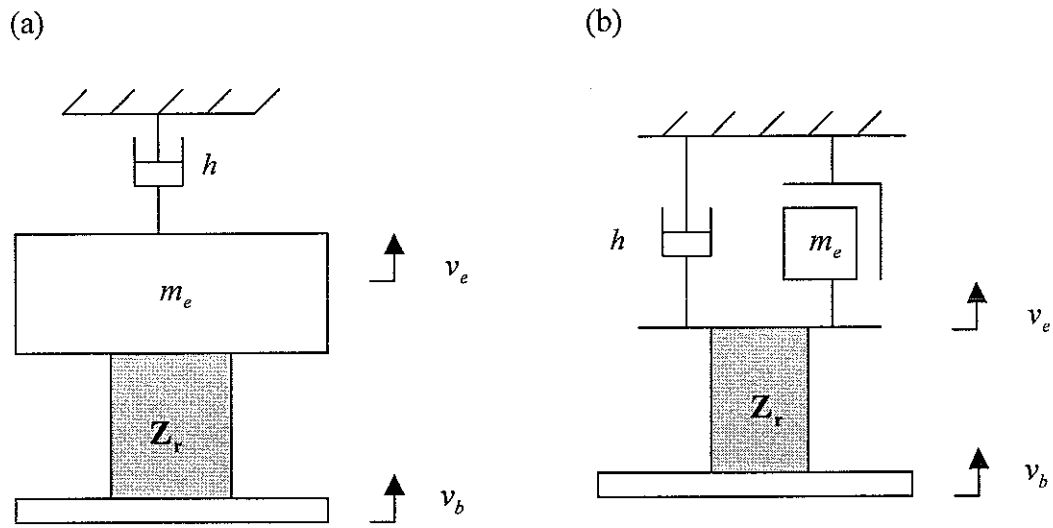

Figure 3.4 Mechanical representation of the absolute velocity feedback control on a system with distributed parameter mount excited by harmonic base motion

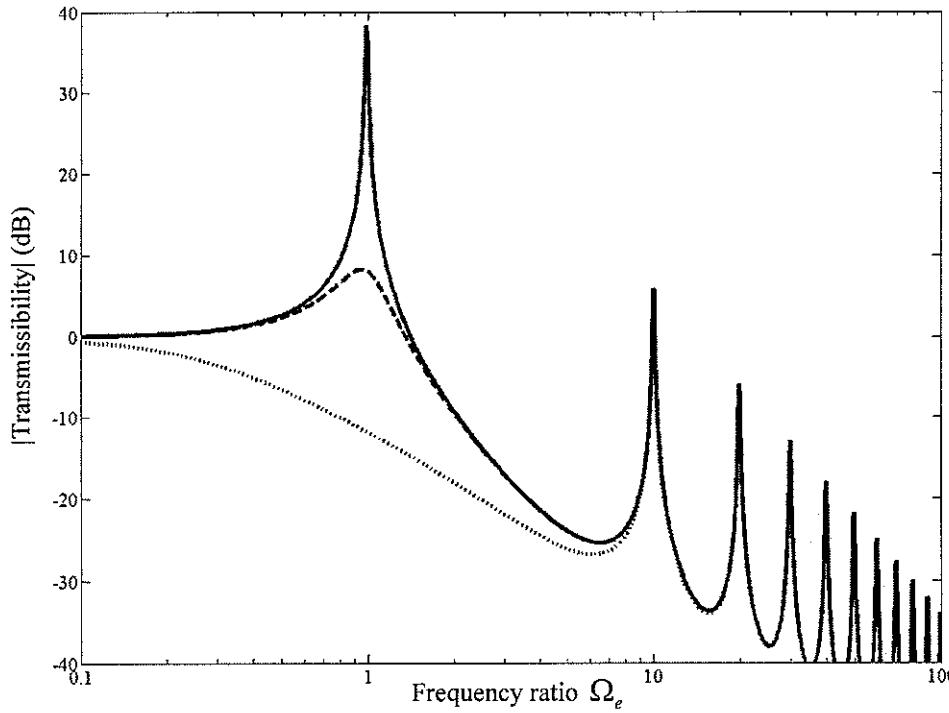

Figure 3.5 Transmissibility of the system with a distributed parameter mount excited by base motion under absolute velocity feedback control with different values of active damping ratio $\zeta_a = 0$ (solid line), $\zeta_a = 0.2$ (dashed line) and $\zeta_a = 2$ (dotted line); $\mu_m = 0.1$, $\eta_m = 0.01$

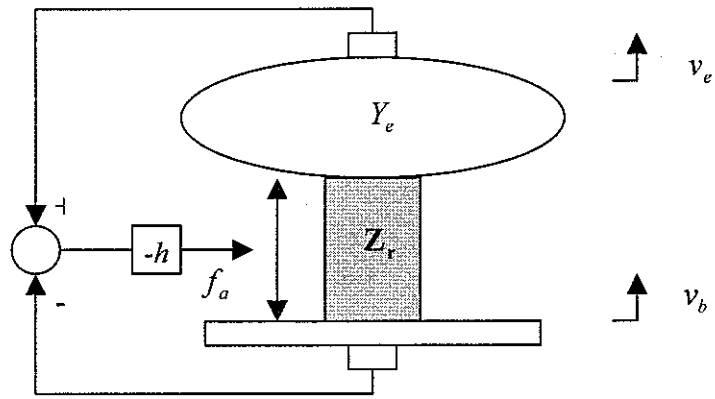

Figure 3.6 Block diagram for the vibrating system with a distributed parameter mount excited by a base motion under RVF control

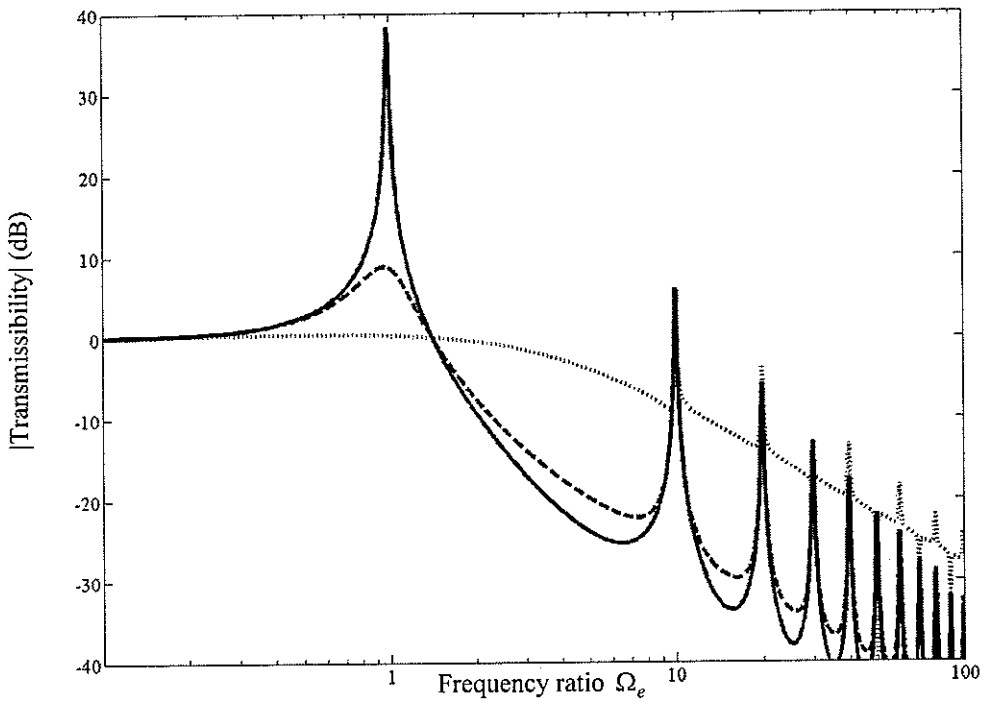

Figure 3.7 Transmissibility of the system with a distributed parameter mount excited by base motion under relative velocity feedback control with different values of active damping ratio $\zeta_a = 0$ (solid line), $\zeta_a = 0.2$ (dashed line) and $\zeta_a = 2$ (dotted line); $\mu_m = 0.1$, $\eta_m = 0.01$

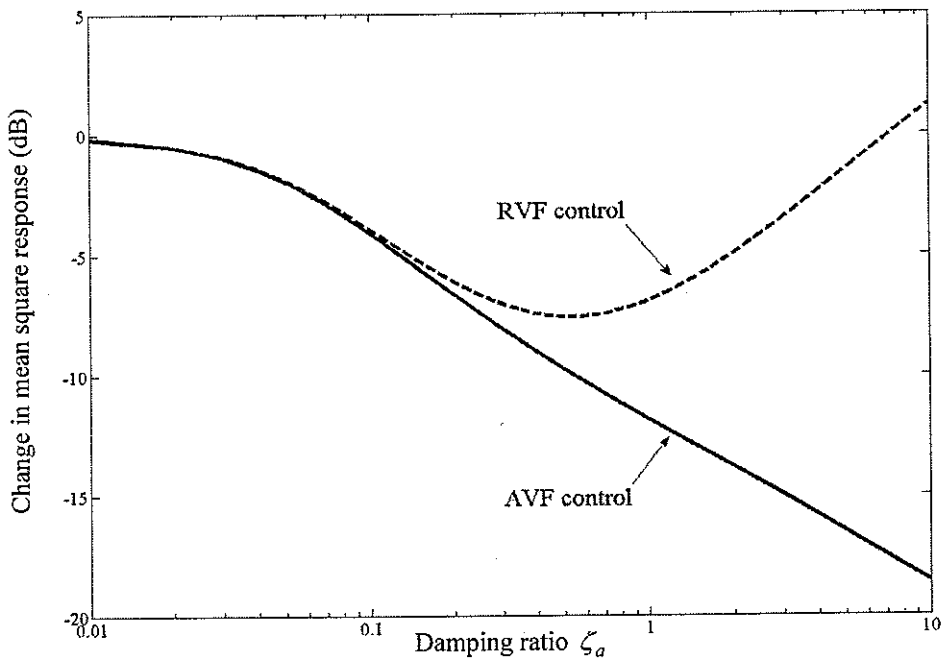

Figure 3.8 Normalised change in mean square displacements compared to the passive system subjected to base excitation for different control strategies, $\mu_m = 0.1$, $\eta_m = 0.01$

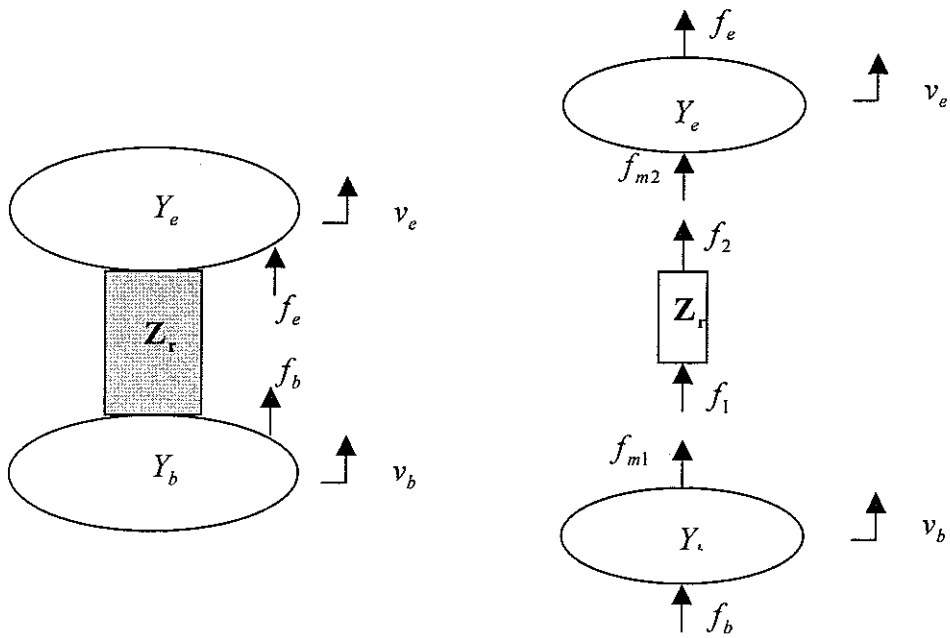

Figure 3.9 Block diagram for the vibrating system with a distributed parameter mount on a flexible base

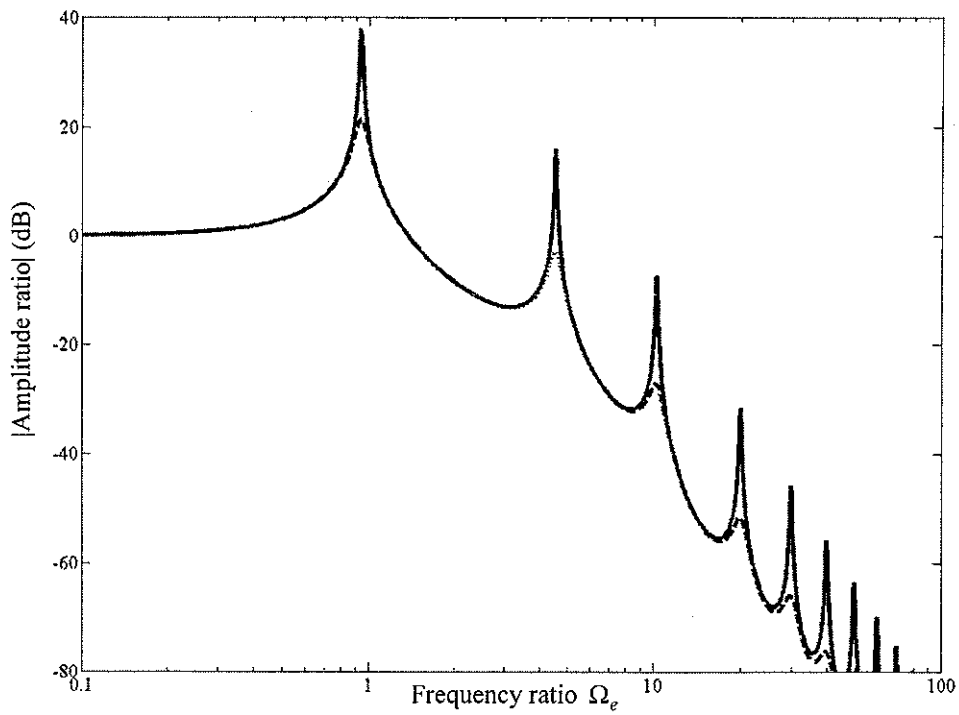

Figure 3.10 Amplitude ratio of the system with a distributed parameter mount on a flexible base when $\mu_m = 0.1, \mu_b = 0.5, \mu_k = 0.1$ and $\eta_m = \eta_b = 0.01$ (solid line), $\eta_m = 0.1, \eta_b = 0.01$ (dashed line), $\eta_m = 0.01, \eta_b = 0.1$ (dotted line), respectively

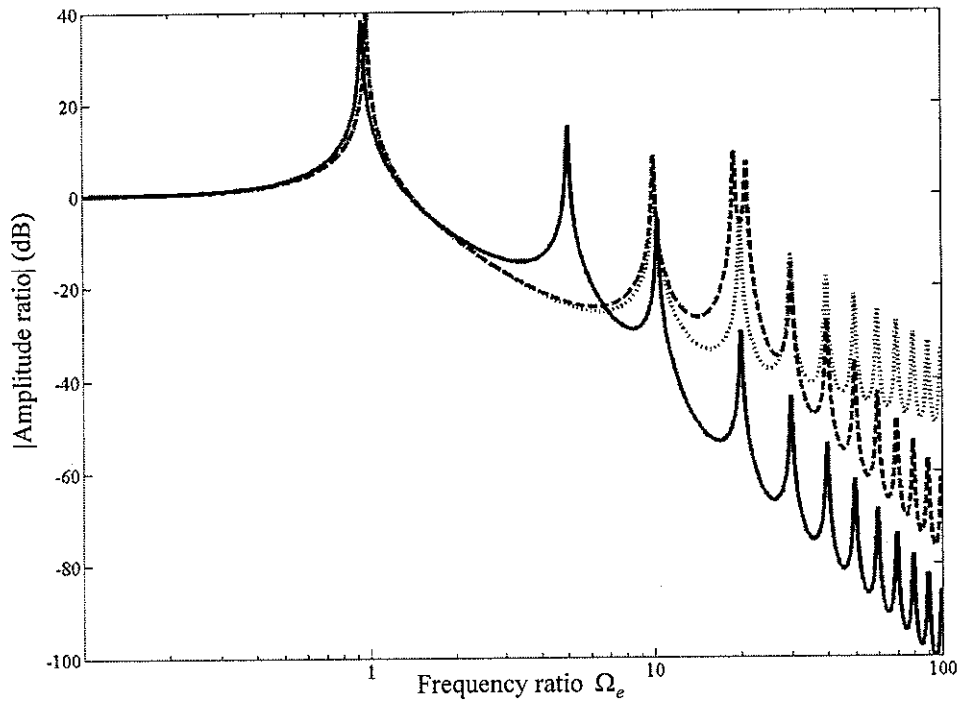

Figure 3.11 Amplitude ratio of the system with a distributed parameter mount on a flexible base when $\mu_m = 0.1$, $\mu_b = 0.5$, $\eta_m = \eta_b = 0.01$ and $\Gamma_b = 5$ (solid line), $\Gamma_b = 20$ (dashed line), $\Gamma_b = \infty$ (dotted line), respectively.

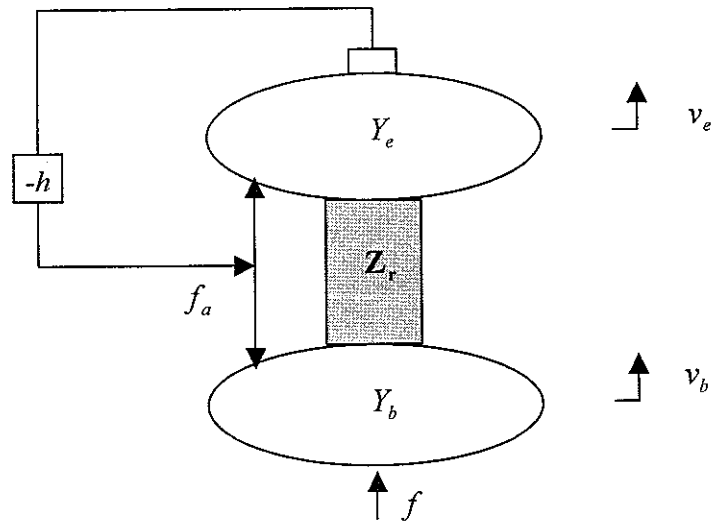

Figure 3.12 Block diagram for the vibrating system with a distributed parameter mount on a flexible base under AVF control

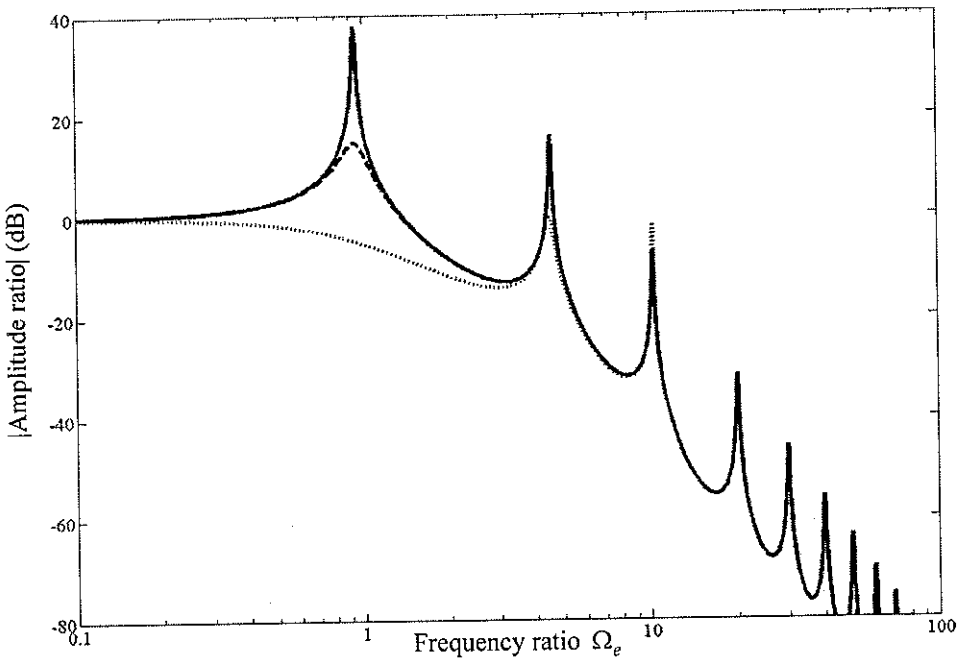

Figure 3.13 Amplitude ratio of the system on a flexible base under AVF control when $\mu_m = 0.1$, $\mu_b = 0.5$, $\mu_k = 0.1$, $\eta_m = \eta_b = 0.01$ and $\zeta_a = 0$ (solid line), $\zeta_a = 0.1$ (dashed line), $\zeta_a = 1$ (dotted line), respectively

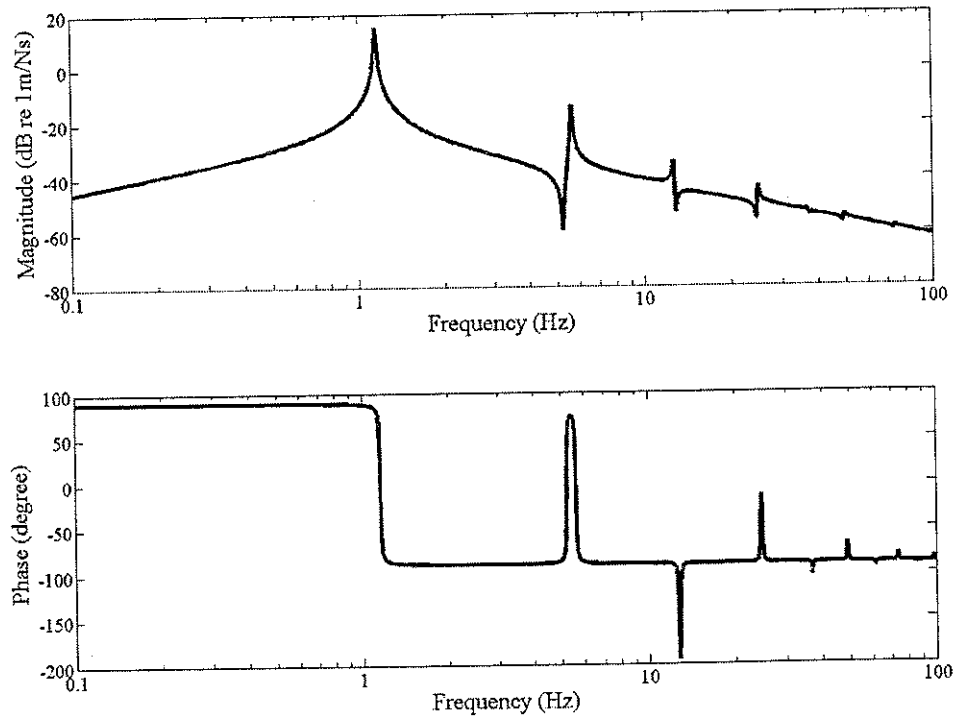

Figure 3.14 Frequency response of the plant response for the system on a flexible base when $\mu_m = 0.1$, $\mu_b = 0.5$, $\mu_k = 0.1$ and $\eta_m = \eta_b = 0.01$

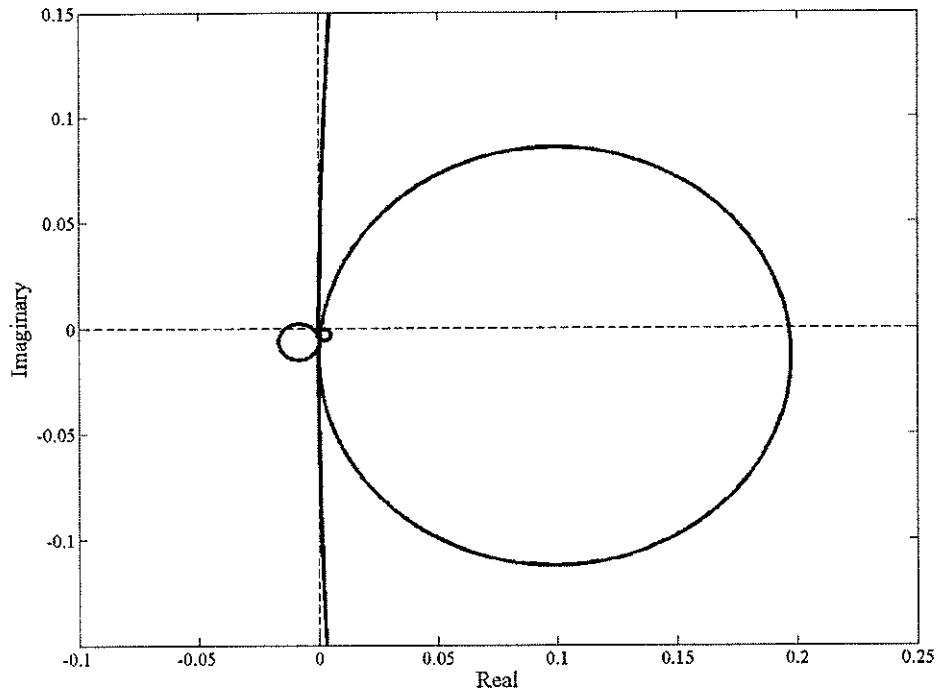

Figure 3.15 Nyquist plot of the plant response for the system on a flexible base when $\mu_m = 0.1$, $\mu_b = 0.5$, $\mu_k = 0.1$ and $\eta_m = \eta_b = 0.01$

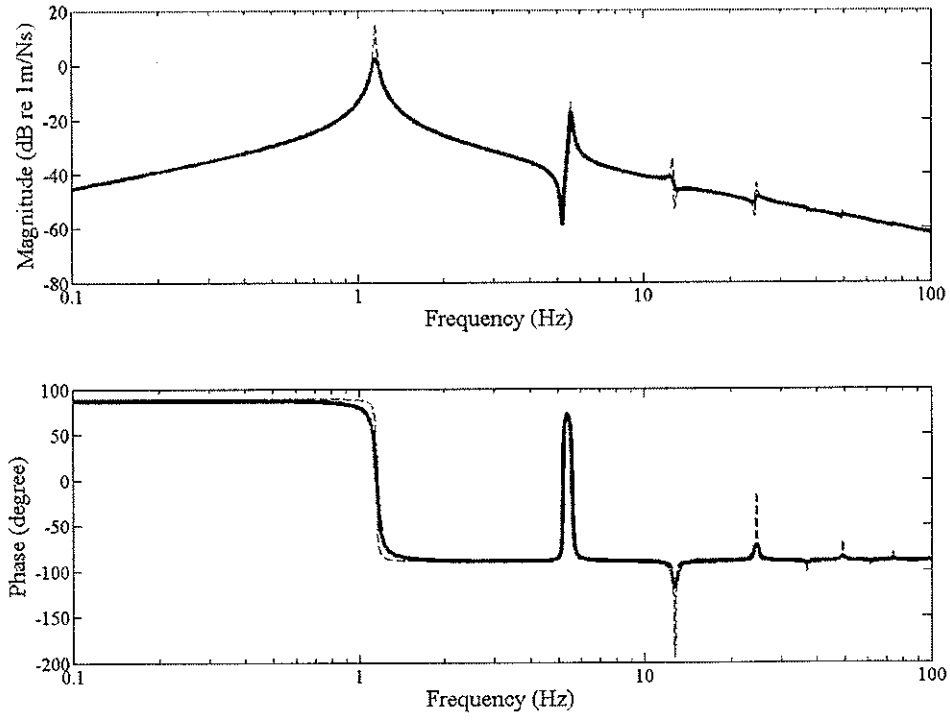

Figure 3.16 Plant frequency response for the system on a flexible base under AVF control when $\mu_m = 0.1$, $\mu_b = 0.5$, $\mu_k = 0.1$, $\eta_b = 0.01$ and $\eta_m = 0.01$ (dashed line), $\eta_m = 0.05$ (solid line), respectively

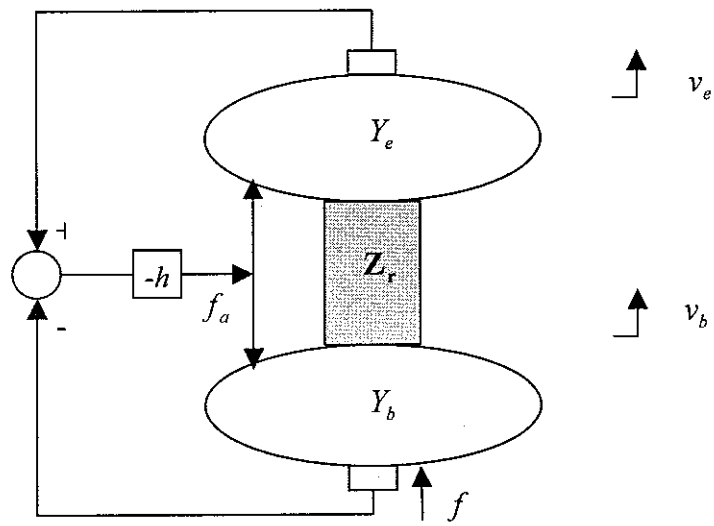

Figure 3.17 Block diagram for the vibrating system with a distributed parameter mount on a flexible base under RVF control

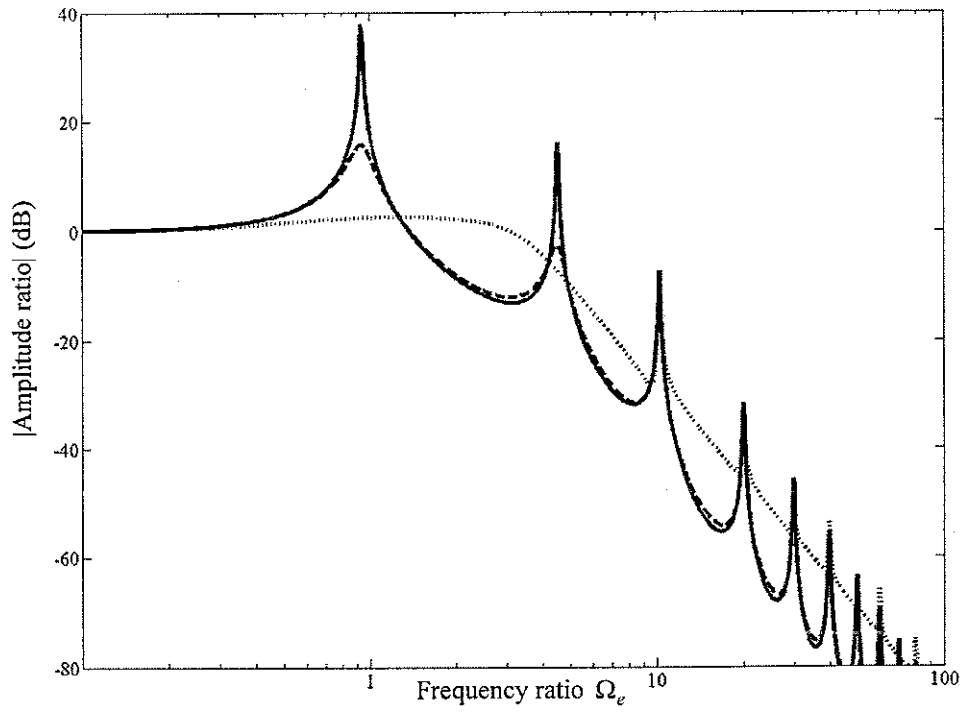

Figure 3.18 Amplitude ratio of the system on a flexible base under RVF control when, $\mu_m = 0.1$, $\mu_b = 0.5$, $\mu_k = 0.1$, $\eta_m = \eta_b = 0.01$ and $\zeta_a = 0$ (solid line), $\zeta_a = 0.1$ (dashed line), $\zeta_a = 1$ (dotted line), respectively

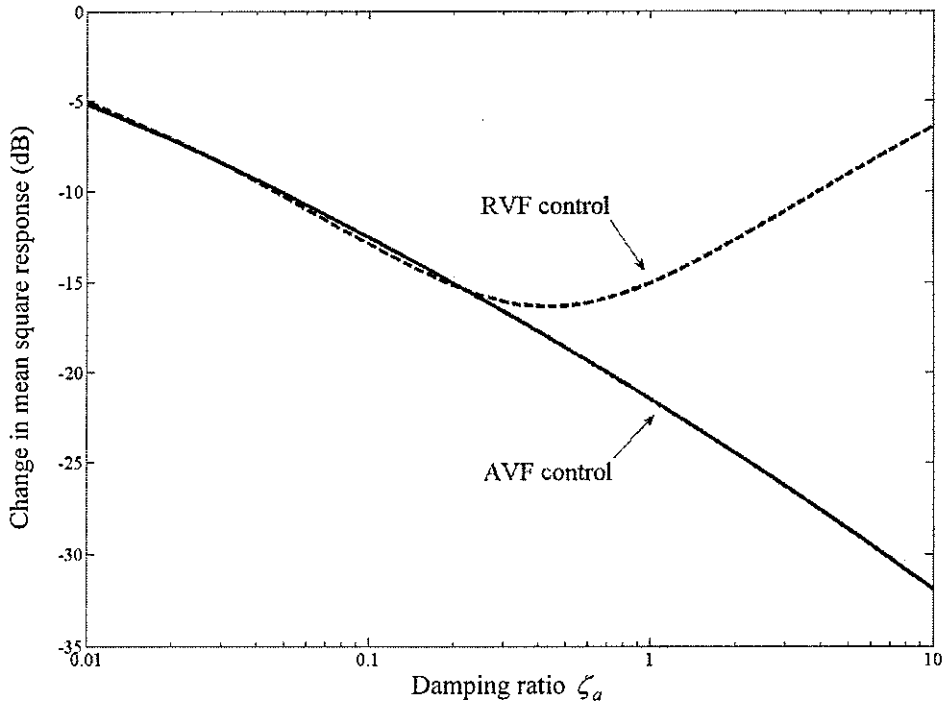

(a)

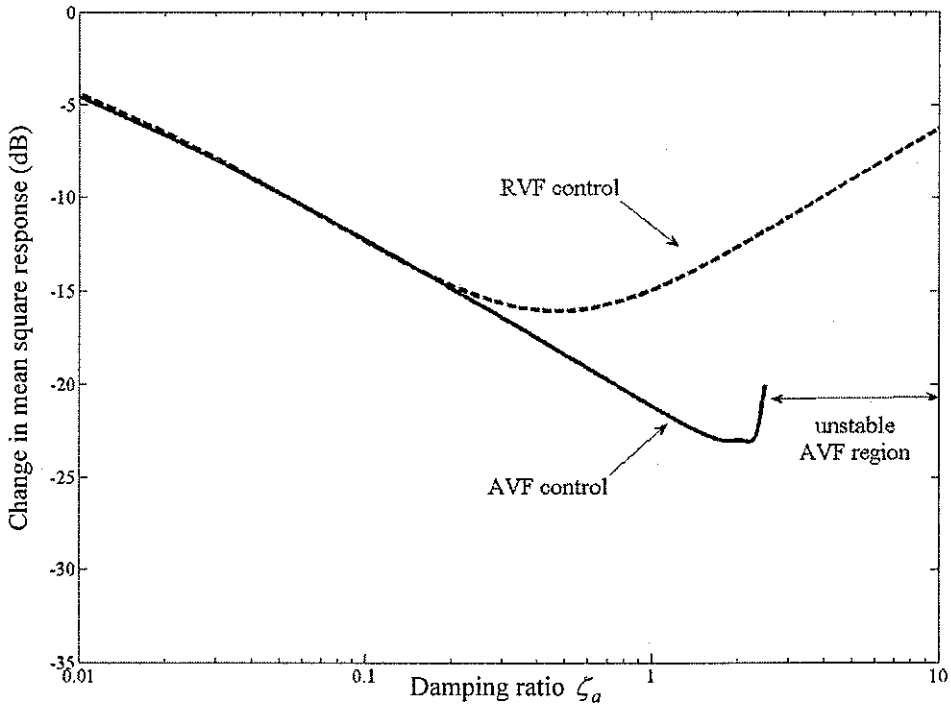

(b)

Figure 3.19 Normalised change in mean square displacements for the system on a flexible base for different control strategies when $\mu_m = 0.1$, $\mu_k = 0.1$, $\eta_m = \eta_b = 0.01$ (a) stable case : $\mu_b = 1$ (b) unstable case: $\mu_b = 0.5$

4 Conclusions

Two different feedback control strategies have been applied to vibration isolation systems consisting of either a lumped parameter isolator or a distributed parameter mount, and the performance and stability of these systems have been investigated.

Undergoing harmonic base motion, the vibration isolation systems with a lumped parameter isolator or a distributed parameter mount are always unconditionally stable under either absolute velocity feedback control or relative velocity feedback control. But the performance of the systems using absolute velocity feedback control is better in that it suppresses the response at the fundamental resonance frequency of the system without compromising passive high frequency isolation.

For the vibration isolation systems on a flexible base with a lumped parameter isolator or a distributed parameter mount, the performance of the systems using absolute velocity feedback control is better also because it suppresses the response of the fundamental resonance frequency of the system without compromising passive high frequency isolation. However the systems need to be carefully designed, as in some situations they are only conditionally stable. For the system with a lumped parameter isolator, instability conditions have been generalized by Elliott et al [9]. In this report, a simple method to determine the stability of the system with a distributed parameter mount in terms of the mode shapes of the system has been proposed. This method can also been applied to the system with a lumped parameter isolator. The maximum control gain is studied in terms of modal damping and mode shapes. This is in contrast to the systems using relative velocity feedback control where the response at the fundamental resonance frequency is suppressed, but there is degradation in the performance of the passive isolator at high frequencies. These systems, however, are unconditionally stable.

Appendix: experiment on a helical spring

To validate the assumption that the distributed parameter mount, whose mass should be considered in practice, can be represented as a finite free-free rod, an experiment on a helical spring has designed.

The mechanical arrangement is illustrated in Figure A.1. A brass cylinder as an equipment, which has a mass, m_e, of 193.1 g is mounted on a mild steel helical spring, which has a density, ρ, of 7800 kg/m^3 and Young's modulus of elasticity, E, of 2×10^{11} N/m^2. The helical spring was excited by a shaker through a force transducer with the connection of a washer, which has a mass, m_b, of 29.2 g. Two accelerometers were located on the equipment and washer, respectively, to measure the acceleration so that the velocity information is aquired.

Therefore, the block diagram of the experiment rig can be represented in the Figure A.2 using the mobility approach. If the helical spring is treated as finite free-free mount, the equations of motion are given by

$$\begin{aligned} v_e &= Y_e f_{m2} \\ v_b &= Y_b\left(f + f_{m1}\right) \\ \begin{bmatrix} f_{m1} \\ f_{m2} \end{bmatrix} &= -\begin{bmatrix} f_1 \\ f_2 \end{bmatrix} = -\mathbf{Z}_r \begin{bmatrix} v_b \\ v_e \end{bmatrix} = -\begin{bmatrix} Z_{11} & Z_{12} \\ Z_{21} & Z_{22} \end{bmatrix}\begin{bmatrix} v_b \\ v_e \end{bmatrix} \end{aligned} \tag{A.1}$$

where $Y_e = 1/j\omega m_e$ is the input mobility of the unconnected equipment at location of the mount connection, $Y_b = 1/j\omega m_b$ is the input mobility of the unconnected mounted washer at the location of the mount connection, $\mathbf{Z}_r$ is the impedance matrix of the finite free-free rod defined in equation (3.1).

Therefore, the transmissibility is given as

$$T = \frac{v_e}{v_b} = -\frac{Y_e Z_{21}}{1 + Y_e Z_{22}} \tag{A.2}$$

Figure A.3 shows the measured and simulated transmissibility, which are well matched, so that it is a good assumption that the distributed parameter mount can be represented as a finite free-free rod.

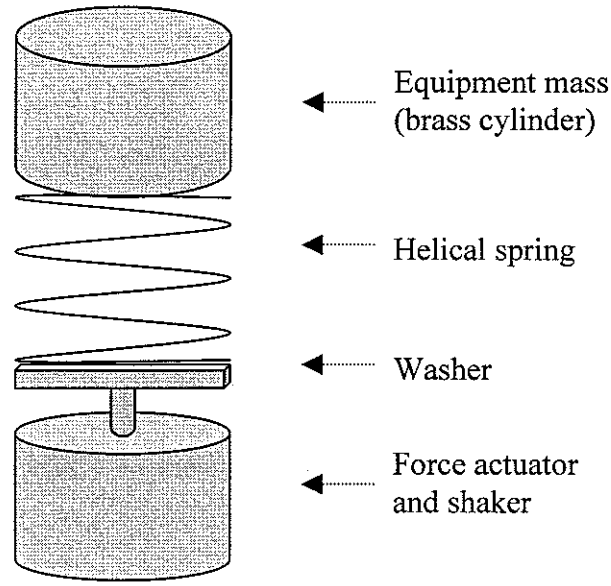

Figure A.1 Physical arrangement of the experiment on a helical spring

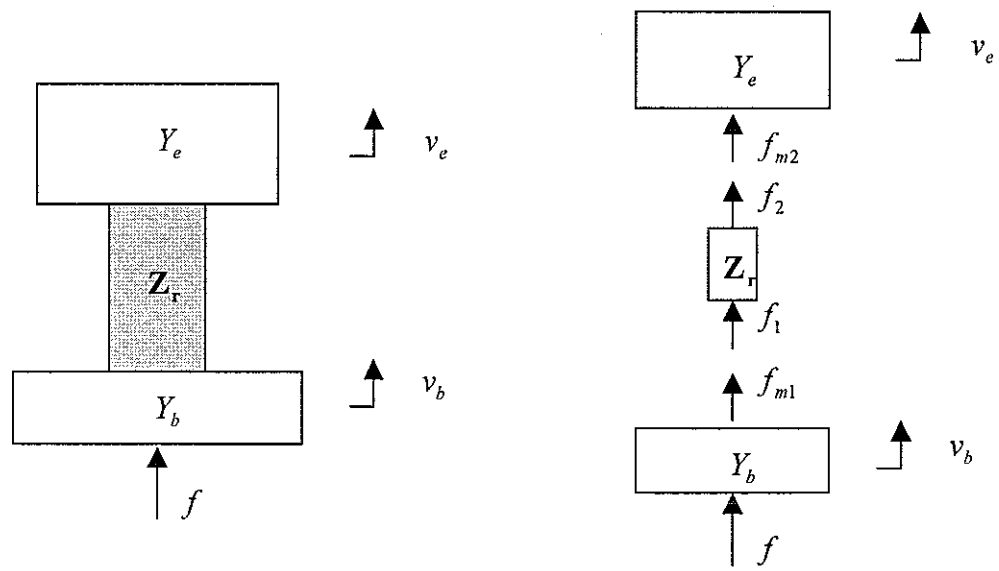

Figure A.2 block diagram for the experiment

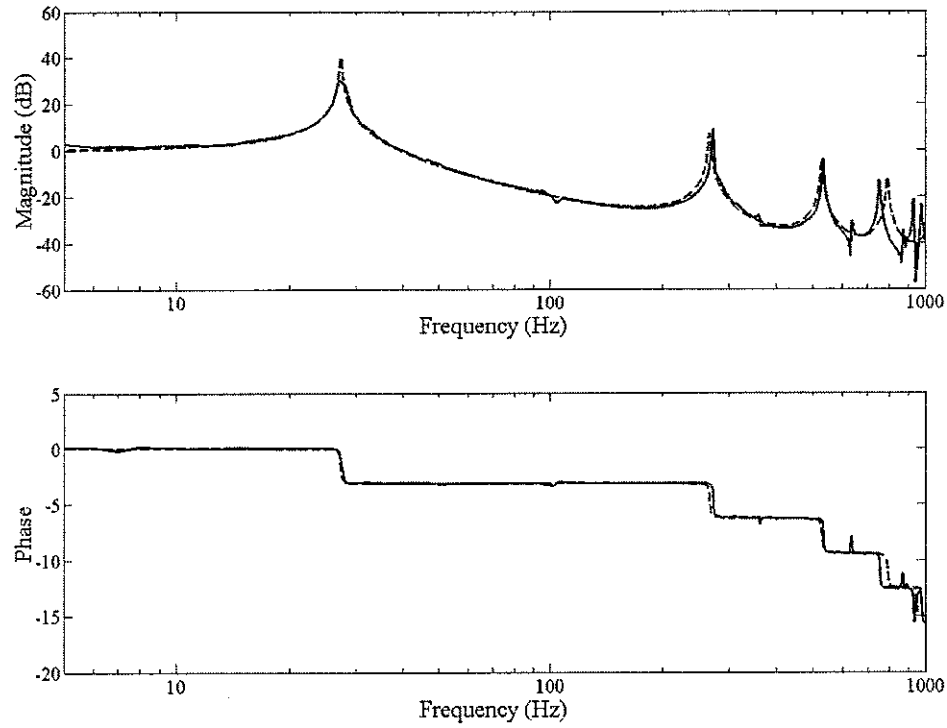

Figure A.3 Measured (solid line) and simulated (dashed line) transmissibility

References

1. Blake, R.E., 2002, Basic vibration theory, Chapter 2, Harris, C.M., and Piersol, A.G., ed., *Shock and Vibration Handbook,* Fifth Edition, McGraw Hill, New York.
2. Rao, S. S., 1984, *Mechanical Vibrations*, Addison-Wesley: Reading, Massachusetts.
3. Thomson, W.T., 1988, Theory of Vibration with Applications, Third Edition, Allen &Unwin, London.
4. Lalor, N., 1998, Fundamentals of vibration, Chapter 2, Fahy, F.J., and Walker, J.G., ed., *Fundamentals of Noise and Vibration,* E&FN SPON, London.
5. Allen, P.W., Lindley, P.B., and Payne, A.R., ed., 1967, Use of Rubber in Engineering, *Proceedings of a Conference held at Imperial College of Science and Technology, London*, Maclaren and Sons LTD, London.
6. Karnopp, D., 1995, Active and semi-active vibration isolation, *American Society of Mechanical Engineers, Journal of Mechanical Design*, **177**, 177-185.
7. Elliott, S.J., Serrand, M., and Gardonio, P., 2001, Feedback stability limits for active isolation systems with reactive and inertial actuators, *American Society of Mechanical Engineers, Journal of Vibration and Acoustics*, **123**, 250-261.
8. Serrand, M., 2000, Direct velocity feedback control of equipment vibration, MPhil Thesis, University of Southampton.
9. Elliott, S.J., Benassi, L., Brennan, M.J., Gardonio, P., and Huang, X., 2004, Mobility analysis of active isolation systems, *Journal of sound and vibration*, **271**, 297-321.
10. Dutton, K., Thompson, S., and Barraclough, B., 1997, *The Art of Control Engineering*, Harlow, Essex: Addison-Wesley.
11. Richards, R.J., 1979, An introduction to dynamics and control, Longman, New York.
12. Skogestad, S., and Postlethwaite, I., 1996, *Multivariable Feedback Control: Analysis and Design,* Chichester, West Sussex: John Wiley & Sons.

13. Gardonio, P., and Brennan, M.J., 1998, Mobility and impedance methods in structural dynamics, Chapter 9, Fahy, F.J., and Walker, J.G., ed., *Advanced applications in acoustics, noise and vibration*, E&FN SPON, London.
14. Bishop, R.E.D., and Johnson, D.C., 1960, *The Mechanics of Vibration*, Cambridge University Press.
15. Holterman, J., and Vries, T.J.A.de., 2005, Active damping based on decoupled collocated control, *ASME, Transactions on mechatronics,* **10**, 135-145.